

Efficiency-Risk Tradeoffs in Dynamic Oligopoly Markets

– with application to electricity markets

by

Qingqing Huang

B.Eng in Electronic Engineering and BBA in General Business
Management

Submitted to the

Department of Electrical Engineering and Computer Science
in partial fulfillment of the requirements for the
degree of

Master of Science in Electrical Engineering and Computer Science
at the

MASSACHUSETTS INSTITUTE OF TECHNOLOGY

June 2013

© Massachusetts Institute of Technology 2013. All rights reserved.

Author.....
Department of Electrical Engineering and Computer Science
May 22, 2013

Certified by.....
Munther A. Dahleh
Professor
Thesis Supervisor

Accepted by.....
Leslie Kolodziejski
Chairman, Department Committee on Graduate Students

Efficiency-Risk Tradeoffs in Dynamic Oligopoly Markets

– with application to electricity markets

by

Qingqing Huang

Submitted to the Department of Electrical Engineering and Computer Science
on May 22, 2013, in partial fulfillment of the
requirements for the degree of
Master of Science in Electrical Engineering and Computer Science

Abstract

In an abstract framework, we examine how a tradeoff between efficiency and risk arises in different dynamic oligopolistic markets. We consider a scenario where there is a reliable resource provider and agents which enter and exit the market following a random process. Self-interested and fully rational agents can both produce and consume the resource. They dynamically update their load scheduling decisions over a finite time horizon, under the constraint that the net resource consumption requirements are met before each individual’s deadline.

We first examine the system performance under the non-cooperative and cooperative market architectures, both under marginal production cost pricing of the resource. The statistics of the stationary aggregate demand processes induced by the two market architectures show that although the non-cooperative load scheduling scheme leads to an efficiency loss - widely known as the “price of anarchy” - the stationary distribution of the corresponding aggregate demand process has a smaller tail. This tail, which corresponds to rare and undesirable demand spikes, is important in many applications of interest.

With a better understanding of the efficiency-risk tradeoff, we investigate, in a non-cooperative setup, how resource pricing can be used as a tool by the system operator to tradeoff between efficiency and risk.

We further provide a convex characterization of the Pareto front of different system performance measures. The Pareto front determines the tradeoff among volatility suppression of concerned measurements in the system with load scheduling dynamics. This is the fundamental tradeoff in the sense that system performance

achieved by any load scheduling strategies induced by any specific market architectures is bounded by this Pareto front.

Thesis Supervisor: Munther A. Dahleh

Title: Professor

Acknowledgments

The warmest thanks go to my advisor Munther Dahleh and Mardavij Roozbehani for their guidance, understanding, patience, and friendship during my first two years at MIT. They always encouraged me to ask meaningful and interesting questions, to think deeply and to think out of the box, and the great experience of working with them motivates me to move on to my PHD study.

I would also like to thank LIDS, where the great learning environment provides positive feedback to one's insatiable curiosity, and talking to those smart and nice people can make one's worrieness and stress disappear.

Finally, and most importantly, I would like to thank my wonderful parents, for their faith in me, and for their unending love and support.

Contents

1	Introduction	15
2	System Model	21
2.1	Agent Arrival Process	21
2.2	Resource pricing	22
2.3	System State Evolution	23
2.4	Non-cooperative Market Architecture	25
2.5	Cooperative Market Architecture	28
2.6	Welfare Metrics	29
3	Tradeoff Analysis for $L = 2$ Case	33
3.1	Equilibrium Strategy and Optimal Cooperative Strategy	33
3.2	Welfare Impacts	35
3.3	Numerical results	38
4	General L Analysis: Pricing	43
5	General L Analysis: fundamental tradeoff	49
6	Conclusion	55

A Tables	57
B Figures	59
C Proofs	71
C.1 Proof of Proposition 1	71
C.2 Proof of Proposition 2	71
C.3 Proof of Proposition 3	72
C.4 Proof of Proposition 4	73
C.5 Proof of Proposition 5	75
D Supplementary Materials	77
D.1 Market Architecture Variations for $L = 2$	77
D.1.1 Number of Agents	77
D.1.2 Risk Sensitivity	79
D.2 Numerical Study of Classes of Linear Load Scheduling Strategies . . .	82
D.3 Congestion Fee and Degree of Cooperation	84
D.4 Example of state space model of LTI system for $L = 3$	86

List of Figures

B-1	Visualization of agent index $(l, \tau)_t$. For $L = 5$, $\tau = 3$, at time t there are at most 3 agents that will stay in the market for 3 periods. If they indeed arrive at the market, namely $h_3(t) = h_4(t - 1) = h_5(t - 2) = 1$, at time t they are indexed as $(5, 3)_t$, $(4, 3)_t$ and $(3, 3)_t$, seperately. . .	59
B-2	System diagrams	60
B-3	Market efficiency under different load scheduling schemes. System parameters as follows: the number of agent types $L = 2$; uncontrollable load Bernoulli arrival rate $q_1 = 1$; mean and variance of arrival load distribution $\mu_1 = \mu_2 = 10$, $\sigma_1 = \sigma_2 = 11$. The cooperative load scheduling scheme leads to a lower aggregate consumption variance and thus a higher efficiency than that of the non-cooperative load scheduling scheme. This is known as the “price of anarchy” of strategic behavior in non-cooperative game.	61

B-4 Risk under different load scheduling schemes. For any arrival rate q , the stationary distribution of the aggregate demand process has a larger tail under the cooperative market architecture than that under the non-cooperative market architecture. System parameters as follows: the number of agent types $L = 2$; Bernoulli arrival rate $q_1 = q_2 = q$; mean and variance of arrival load distribution $\mu_1 = \mu_2 = 15$, $\sigma_1 = \sigma_2 = 4$ 62

B-5 Sample paths of the aggregate demand process under the cooperative and the noncooperative load scheduling schemes. At a smaller time scale, the cooperative load scheduling can better smooth out the aggregate demand process. However, at a larger time scale, there are more demand spikes produced endogenously by the cooperative load scheduling scheme. This is consistent with the observation of “low variance, high tail probability” of aggregate demand stationary distribution under the cooperative market architecture. System parameters as follows: the number of agent types $L = 2$; Bernoulli arrival rate $q_1 = q_2 = 0.9$; mean and variance of arrival load distribution $\mu_1 = \mu_2 = 15$, $\sigma_1 = \sigma_2 = 6$ 63

B-6 Empirical distribution of the stationary aggregate demand process under the cooperative and the noncooperative load scheduling schemes. The stationary distribution under the non-cooperative market architecture is more spread out but also has a smaller tail probability, while the distribution under the cooperative market architecture is more concentrated around the mean but also has a larger tail probability. System parameters as follows: the number of agent types $L = 2$; Bernoulli arrival rate $q_1 = q_2 = 0.6$; mean and variance of arrival load distribution $\mu_1 = \mu_2 = 15, \sigma_1 = \sigma_2 = 6$ 64

B-7 Observations of when spikes happen. The extremely high aggregate demand (demand spikes) happen mostly when the flexible loads are absent and when the aggregate backlog state is high. Here we have $L = 2, \mathbf{D} \sim \mathcal{N}(0, \mathbf{I})$ 65

B-8 The three-way Pareto front. The three objectives are $\|z_1\|_2^2, \|z_2\|_2^2$, and $\|z_3\|_2^2$, which are the variance of the aggregate demand, the aggregate backlog, and the aggregate load mismatch upon deadline, correspondingly. Parameters: $L = 5$ 66

B-9 Visualization of the three-way tradeoff Pareto front. The constraint on one performance measure affects the location of the tradeoff curve of the other two measures. Parameters: $L = 5$ 67

B-10 Efficiency-risk tradeoffs as a result of different market architectural properties, in the case with $L = 2$ 68

B-11 Degree of cooperation leads to efficiency-risk tradeoff. As the system operator increases the “congestion fee” by increasing α , the payoff externality is reduced, and the degree of cooperation increases, leading to a higher efficiency and lower level of robustness. 69

B-12 Empirical distribution of the stationary aggregate demand process under the constraint that the instantaneous demand from any agent is restricted to be non-negative. System parameters as follows: the number of agent types $L = 2$; Bernoulli arrival rate $q_1 = q_2 = 0.6$; mean and variance of arrival load distribution $\mu_1 = \mu_2 = 15$, $\sigma_1 = \sigma_2 = 6$. Under the bounded constraint. Observations similar to that for Figure B-6 can be made. 70

List of Tables

A.1 Notations 57

Chapter 1

Introduction

Load scheduling, i.e., optimizing the demand for a resource over multiple periods to minimize the expected total cost of consumption, plays a crucial role in a wide array of applications, including dynamic demand response to realtime prices in electricity markets [6, 22], load scheduling in cloud computing under QoS constraints [4, 17, 3], and multi-period rebalancing of multiple portfolio accounts in the presence of transaction costs [25]. In many cases where the price per unit resource in each period is determined by the instantaneous aggregate demand of finitely many agents, the problem falls into the category of dynamic oligopolistic competition [18, 16].

In a multi-agent system, profit-seeking agents try to maximize their own utilities, by forming rational expectations over the behaviors of other agents, and responding to instantaneous changes in the environment. The agent load scheduling scheme at equilibrium is shaped by different features of the oligopolistic market architecture, including whether the agents are able to cooperate in decision making, including the risk sensitivity of the agents, and including how their costs are coupled, namely, the rule that the price is determined. From a system operator's perspective, the

impact of the aggregate behavior of rational agents is nontrivial – on one hand, it determines the system efficiency, and on the other hand, agent interactions can lead to endogenous risk. For example, in electricity markets, aggregate demand spikes can incur additional costs to the resource provider or the power system as a whole. We shall focus on the measure of risk that quantifies such aggregate demand spikes, and examine how they may arise from the market architectural properties.

In many complex systems with interactive agents, for example, power networks, financial markets, social networks, and biological networks, the mechanisms that can possibly channel exogenous shocks into endogenous risk are still not well understood. Previous research efforts have explored various possible origins of endogenous risk. The notion of “endogenous risk” in financial market was introduced in [8, 9]. When homogeneous traders with trading limits start to sell as the price decreases, their failure to endogenize other traders’ actions leads to price fluctuation and instability. The authors argue that ignoring the feedback link from traders’ actions to the market price can damage the financial market in this way. Other research efforts that attempted to explain the fluctuations in financial market have examined information asymmetry [5], bounded rationality [21] and heterogeneous beliefs [11]. In our work, we assume rational agents, who are fully aware of the pricing mechanism, have complete information about other agents in the market, and form rational expectations. In this work, we provide an alternative explanation through a comparative study, and posit that endogenous risks can arise from the nature of the system dynamics even at a complete information rational expectation equilibrium (REE).

We create an abstract dynamic framework to model agents’ response to realtime costs in the form of load scheduling with deadline constraints, and we investigate the impact of aggregate behavior on system performance, with the hope of finding behaviors and properties that transcend the abstraction of the model. We first examine

the system performance under the non-cooperative and cooperative market architectures, both with marginal production cost pricing of the resource so that agents' demands for the resource are strategic substitutes. Under the non-cooperative market architecture, the load scheduling problem is formulated as a stochastic dynamic oligopolistic game, and under the cooperative market architecture, it is formulated as an infinite-horizon average-cost Markov decision problem (MDP). We shall focus on two performance measures: market efficiency and the risk of aggregate demand spikes. In the non-cooperative market, each agent schedules his consumption to optimize his expected cost of implementing his schedule; in the cooperative market, the agents cooperate in the decision making process to optimize aggregate expected cost. We observe that under the cooperative market architecture, the agents are more aggressive in absorbing exogenous uncertainties, and they can achieve higher market efficiency, i.e., lower cost on average. However, the tradeoff is a higher endogenous risk in terms of a higher probability of aggregate demand spikes. We also show that across load scheduling strategies induced by various oligopolistic market architectures, there exists a tradeoff between efficiency and risk.

With a better understanding of the origin of the aggregate demand spikes, we facilitate the analysis by focusing on the linear time-invariant part of the system dynamics and defining the substitute performance measures. In the linear time-invariant framework, we examine how the pricing rule can be used to induce the desired agent behavior in a non-cooperative market. Moreover, we characterize the Pareto front of system performance measures, which describes the fundamental tradeoff limit for the system with the load scheduling dynamics. The implication of our efficiency and risk analysis is that when the system architecture and operational policies are designed, system efficiency should not be the only goal that is pursued; endogenous risk and the associated tradeoffs should also be carefully considered.

An interesting example where we can apply the analytical framework to study the efficiency-risk tradeoffs is the dynamic demand response to realtime prices in electricity markets in the form of scheduling flexible loads. On the supply side, the intermittency of the renewable sources introduces exogenous supply shocks. On the demand side, large or perhaps small consumers may be able to actively respond to the realtime electricity prices. A considerable amount of the consumer response will take the form of scheduling flexible loads, for example, electrical vehicle charging, building heating, and industrial processing [1, 15, 20]. A specific example of electrical vehicle charging where our framework fits can be found in [10]. We model the market participation behavior of both the consumers and the distributed renewable generations, with potential load scheduling and storage techniques. The resulting dynamic demand supply interaction can better model future smart grids. Consumer participation in smart grids is modeled in a similar way in [7], but the heterogeneous deadline constraints of individual players, which are essential in producing the aggregate demand spikes in our framework, are not modeled explicitly there. However, this is important, as in electricity markets, exceedingly large demand and/or price spikes introduce a level of volatility that can not only cause serious economic damage to both the reliable service provider and consumers, but also undermine viability of power markets as a whole.

The remainder of the thesis unfolds as follows. In Chapter 2, we introduce the system model and formulate the problem; in Chapter 3, we focus on a specific case for which analytical solutions are obtained, and examine how various architectural properties affect the efficiency-risk tradeoffs; in Chapter 4, we introduce the linear time-invariant framework, and discuss how the system operator's decision on the pricing rule will affect agent load scheduling behavior in a non-cooperative setup; in Chapter 5, we provide a convex characterization of the Pareto front of performance

measures, which dictates the fundamental tradeoff of the system with load scheduling dynamics; in Chapter 6, we conclude the paper with a discussion about future work.

Chapter 2

System Model

In this chapter we introduce the general system model consisting of heterogeneous agents which arrive at the system following a random arrival process, a reliable resource provider and a marginal cost pricing mechanism. We also define the non-cooperative and cooperative market architectures.

2.1. Agent Arrival Process

We analyze a market model in which the agent arrival process is a discrete time random process with time intervals indexed by $t = 0, 1, 2, \dots$. When an agent arrives, he activates a job that requires consuming a certain amount of the resource to complete. The agent has to finish the job within a finite window of time, and leave the market at his deadline. We define the number of periods that an agent stays in the market to be his *type*, denoted by $l \in \mathcal{L} = \{1, \dots, L\}$. We assume that agents of type l arrive according to a Bernoulli process $\{h_l(t) : t \in \mathbb{Z}\}$, with rate q_l . Upon arrival at the beginning of period t , an agent carries a job which requires $d_l(t)$

units of the resource in total. We assume that the sequence $\{d_i(t) : t \in \mathbb{Z}\}$ is i.i.d., drawn from a general distribution D_i with mean $\mu_i = \mathbb{E}[D_i]$, variance $\sigma_i^2 = \text{Var}[D_i]$, and with support over the set of all real numbers \mathbb{R} . Let the L -dimensional column vectors $\mathbf{h}(t) = [h_i(t)] \in \{0, 1\}^L$, and $\mathbf{d}(t) = [d_i(t)] \in \mathbb{R}^L$ denote the vector forms of arrival events and the corresponding workloads. Let $U(t)$ denote the instantaneous aggregate demand for the resource from all agents in the market. The key notations that we will introduce throughout the paper are listed in Table A.1.

Remark 1 *Note that for the convenience of our analysis, we allow the load realizations as well as the instantaneous resource demand from the agents to become negative. This models the situation where distributed agents can be both suppliers and consumers in the market. In financial market, the informed traders can be both buyers and sellers, and the uninformed traders have a passive role which is similar to the reliable resource provider [13]. In electricity markets, this corresponds to the scenario where consumers are equipped with distributed renewable generations or pumped-storage units, and are able to sell energy back to the power grid. We ran extensive numerical simulations for the scenario where there is a lower bound on instantaneous resource demand and/or supply. In particular, when the lower bound equals zero, the agents are only consumers and cannot supply the resource to the market. In all of our the simulations, the main results hold qualitatively.*

2.2. Resource pricing

We assume that there is a reliable resource provider which always produces enough amount of the resource to meet the aggregate demand in each period. Moreover, we assume that the production cost borne by the provider is of quadratic form $\frac{1}{2}U(t)^2$,

and the price per unit resource, $p(t)$, is set to be the marginal cost of production in each period, thus $p(t) = U(t)$. We adopt quadratic cost functions for two reasons: firstly they constitute second-order approximation to other types of nonlinear cost functions, and secondly they are analytically tractable, with which closed-form solutions can hopefully provide insights into more general system dynamics. Also, note that the quadratic cost function only models the production cost of the reliable resource provider, which we assume to have no intertemporal constraints. Overall, the aggregate demand is satisfied by the sum of distributed supplies from the agents, and the resource produced by the reliable resource provider. The price is set to provide sufficient incentive to the reliable resource provider to produce at the level where the overall production matches the aggregate consumption. In electricity markets, marginal cost pricing is a widely used mechanism [23]. When both the suppliers and consumers are price takers and there is no intertemporal ramping cost, marginal cost leads to social optimality. Moreover, the reliable resource provider corresponds to the conventional electricity generations which provide reliable electricity, as opposed to the distributed renewable generations, which are stochastic in the nature.

2.3. System State Evolution

At any period t , we group the agents by their departure times. For any $\tau \in \mathcal{L}$, there are at most $(L + 1 - \tau)$ agents who will stay in the market for τ periods (including t). They correspond to the type τ arrival at time t , the type $(\tau + 1)$ arrival at time $(t - 1)$, etc. Take $L = 5$, $\tau = 3$ as an example. Figure B-1 shows that at time t there are 3 possible agents who will stay in the market for $\tau = 3$ periods. For notational convenience, we index a type l agent who at time t will continue to stay in the market

for τ periods by a tuple $(l, \tau)_t$, and we list all possible (l, τ) tuple in the ordered set:

$$\begin{aligned} \mathcal{C} = \{ & (1, 1), (2, 1), (3, 1) \cdots, (L, 1), \\ & (2, 2), (3, 2), \cdots, (L, 2), \\ & \cdots, (L, L). \} \end{aligned}$$

Let $D_c = L(L + 1)/2$ denote the cardinality of the ordered set \mathcal{C} . Let $u_{(l,\tau)}(t) \in \mathbb{R}$ denote the *instantaneous demand* from agent $(l, \tau)_t$, with the vector form denoted by:

$$\mathbf{u}(t) = [u_{(l,\tau)}(t) : (l, \tau) \in \mathcal{C}] \in \mathbb{R}^{D_c}.$$

If at time t there is no agent $(l, \tau)_t$, i.e., $h_l(t + \tau - l) = 0$, we simply define $u_{(l,\tau)}(t) = 0$. The instantaneous aggregate demand is therefore $U(t) = \sum_{(l,\tau) \in \mathcal{C}} u_{(l,\tau)}(t) = \mathbf{1}'\mathbf{u}(t)$, where $\mathbf{1}$ is a D_c -dimensional column vector of all ones. Similarly, we define the *backlog state* $\mathbf{x}(t)$ and the *existence state* $\mathbf{o}(t)$ as follows:

$$\mathbf{x}(t) = [x_{(l,\tau)}(t) : (l, \tau) \in \mathcal{C}] \in \mathbb{R}^{D_c}, \quad (2.1)$$

$$\mathbf{o}(t) = [o_{(l,\tau)}(t) : (l, \tau) \in \mathcal{C}] \in \{0, 1\}^{D_c}, \quad (2.2)$$

where element $x_{(l,\tau)}(t)$ denotes agent $(l, \tau)_t$'s unsatisfied load at time t , and element $o_{(l,\tau)}(t) = 1$ if and only if there is an arrival of type l agent at time $(t + \tau - l)$. Finally, system state at time t is defined to be $\mathbf{s}(t) = (\mathbf{x}(t), \mathbf{o}(t)) \in \mathcal{S}$, where $\mathcal{S} = \mathbb{R}^{D_c} \times \{0, 1\}^{D_c}$ is the state space. We assume that system state is updated after the realization of $\mathbf{h}(t)$ and $\mathbf{d}(t)$ at the beginning of each period t , and the state information is publicly available to all agents in the market¹. The system state

¹ We acknowledge that this complete information assumption is very strong in real life applications with autonomous agents, especially when the number of agents is large. Information structure,

$\mathbf{s}(t) = (\mathbf{x}(t), \mathbf{z}(t))$ evolves as follows:

$$\mathbf{x}(t+1) = \mathbf{R}_1(\mathbf{x}(t) - \mathbf{u}(t)) + \mathbf{R}_2\mathbf{d}(t) \quad (2.3)$$

$$\mathbf{o}(t+1) = \mathbf{R}_1\mathbf{o}(t) + \mathbf{R}_2\mathbf{h}(t) \quad (2.4)$$

where \mathbf{R}_1 is a $D_c \times D_c$ matrix with non-zero elements:

$$\mathbf{R}_1\left((k-1)\left(L + \frac{2-k}{2}\right) + i + 1, \quad k\left(L + \frac{1-k}{2}\right) + i\right) = 1,$$

for all $1 \leq i \leq L - k$ and $1 \leq k \leq L - 1$,

and all other elements being 0. Also, \mathbf{R}_2 is a $D_c \times L$ matrix with non-zero elements:

$$\mathbf{R}_2\left((l-1)\left(L + \frac{2-l}{2}\right) + 1, \quad l\right) = 1, \text{ for all } 1 \leq l \leq L.$$

and all other elements being 0. As an example, the matrices \mathbf{R}_1 and \mathbf{R}_2 for $L = 3$ are given in Appendix D.4.

2.4. Non-cooperative Market Architecture

We define the *non-cooperative market architecture* to be a market setup in which there is no coordination among the strategic agents in scheduling their loads. With full information about the system model and the state evolution $\{\mathbf{s}(t') : t' \leq t\}$, an agent $(l, \tau)_t$ makes the decision of his instantaneous resource demand $u_{(l,\tau)}(t)$ based on his observation of system state $\mathbf{s}(t)$. We assume that the agents do not directly

though an important issue in dynamic games, is not the focus of this paper, as the identified mechanism that produces endogenous risk of spikes also exists in incomplete information models. This simplification assumption affords us a model which is tractable and can serve as a benchmark for incomplete information models.

derive utility from consumption of the resource. Thus the only objective they have is to minimize the expected total cost, under the constraint that each agent's total consumption by his deadline must be equal to his workload. Note that compared to the standard modeling of utility as an increasing function in consumption, this is a more accurate modeling of consumer behavior in terms of decision making about electricity consumption. Our framework can also be extended to cases where agents value their consumptions. For example, later in Chapter 5, we shall relax the deadline constraints, while including the disutility from the mismatch between real consumptions and the target consumption to complete the tasks into agent payoff function.

More specifically, under the non-cooperative architecture, a type l agent who arrives at time t dynamically optimizes his consumption schedule $\{u_{(l,l-i)}(t+i) : i = 0, 1, \dots, l-1\}$ to minimize his expected payment $\mathbb{E}[\sum_{i=0}^{l-1} p(t+i)u_{(l,l-i)}(t+i)]$. Due to the cost coupling through endogenous pricing, we model agent interaction by a stochastic dynamic game, with the following specification:

- **Players:** Over infinite time horizon, the players are indexed by $\{(l, \tau)_t : t \in \mathbb{Z}, (l, \tau) \in \mathcal{C}\}$ according to their type and arrival time in the market.
- **State Space:** The state space is given by \mathcal{S} .
- **Action Set:** The action set is given by \mathcal{A} . In particular, the action set of player $(l, \tau)_t$ at time t in state \mathbf{s} is given by:

$$A_{(l,\tau)}(\mathbf{s}) = \begin{cases} 0, & \text{if } z_{(l,\tau)} = 0 \\ x_{(l,\tau)}, & \text{if } z_{(l,\tau)} = 1 \text{ and } \tau = 1 \\ \mathbb{R}, & \text{otherwise} \end{cases} \quad (2.5)$$

- **Transition Probability:** For each state \mathbf{s} and action vector $\mathbf{u} \in \prod_{(l,\tau)} A_{(l,\tau)}(\mathbf{s})$,

the transition probability $\mathbb{P}(\mathbf{s}'|\mathbf{s}, \mathbf{u})$ is consistent with the state dynamics in (2.3), (2.4) and the agent arrival process in 2.1.

We shall focus on *Markov Perfect Equilibrium* (MPE) [24, 19] throughout our discussion. This refers to a subgame perfect equilibrium of the stochastic dynamic game where players' strategies only depend on the current state. The *Markov strategy* is thus defined as a function:

$$\mathbf{u} : \mathcal{S} \rightarrow \mathcal{A}$$

which maps the system state to the instantaneous demand in the action set from agent $(l, \tau)_t$. Moreover, as all agents have the same cost structure, it is natural to focus on symmetric stationary pure strategy equilibria where for every $(l, \tau) \in \mathcal{C}$, the agents $\{(l, \tau)_t : t \in \mathbb{Z}\}$ adopt the same decision rule denoted by $\mathbf{u}(\mathbf{s})$. The symmetry of this problem makes it possible to consider a single agent's problem to characterize the equilibrium, which we formalize as follows:

Definition 1 (Markov Perfect Symmetric Equilibrium Strategy) *A strategy profile*

$$\mathbf{u}^{nc} = \{u_{(l,\tau)}^{nc}(\mathbf{s}) : (l, \tau) \in \mathcal{C}, \mathbf{s} \in \mathcal{S}\}$$

is defined to be a Markov Perfect Symmetric Equilibrium Strategy, if the following fixed point equations are satisfied for all agents $(l, \tau) \in \mathcal{C}$ at any time t , for any system states $\mathbf{s}(t) \in \mathcal{S}$:

$$u_{(l,\tau)}^{nc}(\mathbf{s}(t)) = \arg \min_u \mathbb{E} \left[p(t)u + \sum_{i=1}^{\tau-1} p(t+i)u_{(l,\tau-i)}^{nc}(\mathbf{s}(t+i)) \middle| \mathbf{s}(t) \right] \quad (2.6)$$

$$\begin{aligned}
\text{subject to: } & \sum_{i=0}^{l-1} u_{(l,l-i)}^{nc}(\mathbf{s}(t+i)) = d_l(t), \quad \forall t, l, \\
& p(t) = u + \sum_{(l',\tau') \in \mathcal{C}, (l',\tau') \neq (l,\tau)} u_{(l',\tau')}^{nc}(\mathbf{s}(t)), \\
& p(t+i) = \sum_{(l',\tau') \in \mathcal{C}} u_{(l',\tau')}^{nc}(\mathbf{s}(t+i)), \quad \forall i \geq 1,
\end{aligned}$$

where $\mathbf{s}(t)$ evolves according to (2.3), (2.4).

2.5. Cooperative Market Architecture

As an efficiency benchmark, we consider the cooperative market architecture, under which the agents can coordinate their actions to minimize their aggregate expected cost. Later, we show that under the assumptions of quadratic production cost and marginal cost pricing, the cooperative market architecture leads to the highest market efficiency, defined as the total surplus from all agents and the reliable resource provider. The cooperative market architecture can model the scenario where the agents agree a priori upon a common strategy that minimizes their aggregate expected cost, and respond to the realtime market conditions according to the pre-specified strategy. Particularly, in future electricity markets, the cooperative scheme may correspond to the situation where the consumers with flexible loads pass all the relevant information to a load aggregator who schedules the loads on their behalf. We are interested in the system performance in the stationary equilibrium, and define the *optimal stationary cooperative strategy* under the cooperative market architecture as follows:

Definition 2 (Optimal Stationary Cooperative Strategy) *A strategy profile*

$$\mathbf{u}^c = \{\mathbf{u}_{(l,\tau)}^c(\mathbf{s}) : (l, \tau) \in \mathcal{C}, \mathbf{s} \in \mathcal{S}\}$$

is defined to be an *Optimal Stationary Cooperative Strategy* if $\mathbf{u}^c(\mathbf{s}) = [u_{(l,\tau)}^c(\mathbf{s}) : (l, \tau) \in \mathcal{C}]$ solves the following fixed point equations for any system states $\mathbf{s}(t) \in \mathcal{S}$:

$$\mathbf{u}^c(\mathbf{s}(t)) = \arg \min_{\mathbf{u}^c = [u_{(l,\tau)} : (l,\tau) \in \mathcal{C}]} \lim_{T \rightarrow \infty} \frac{1}{T-t} \mathbb{E} \left[\sum_{(l,\tau) \in \mathcal{C}} p(t) u_{(l,\tau)} + \sum_{t'=t+1}^T \sum_{(l,\tau) \in \mathcal{C}} p(t+i) u_{(l,\tau)}^c(\mathbf{s}(t')) \middle| \mathbf{s}(t) \right] \quad (2.7)$$

$$\text{subject to: } \sum_{i=0}^{l-1} u_{(l,l-i)}^c(\mathbf{s}(t+i)) = d_l(t), \quad \forall t, l,$$

$$p(t) = \sum_{(l,\tau) \in \mathcal{C}} u_{(l,\tau)},$$

$$p(t+i) = \sum_{(l,\tau) \in \mathcal{C}} u_{(l,\tau)}^c(\mathbf{s}(t+i)), \quad \forall i \geq 1,$$

where $\mathbf{s}(t)$ evolves according to (2.3), (2.4).

The above problem is a standard infinite horizon average cost MDP, and the associated Bellman equation can be solved via standard value iteration or policy iteration [2].

2.6. Welfare Metrics

Different oligopolistic market architectures induce different agent behaviors, which lead to different stationary distributions of the aggregate demand process $\{U(t) : t \in \mathbb{Z}\}$. We shall focus on two welfare metrics: **efficiency** and **risk**. More specifically,

we define *efficiency* to be the expected sum of the resource provider's surplus W_p and the agents' surplus W_a as follows:

$$W = \underbrace{\mathbb{E}[p(t)U(t) - \frac{1}{2}U(t)^2]}_{W_p} + \underbrace{\mathbb{E}[-p(t)U(t)]}_{W_a} = -\frac{1}{2}\mathbb{E}[U(t)^2] = \frac{1}{2}W_a \quad (2.8)$$

Note that under the assumptions of quadratic production cost and marginal cost pricing, efficiency is decreasing in $\mathbb{E}[U(t)^2]$. In (2.7), the optimal stationary cooperative strategy $\mathbf{u}^c(\cdot)$ maximizes W_a , thus achieves the highest efficiency in the sense of (2.8), which we denote by $W^c = W_p^c + W_a^c$. Let $W^{nc} = W_p^{nc} + W_a^{nc}$ denote the efficiency achieved by the equilibrium strategy $\mathbf{u}^{nc}(\cdot)$ under the non-cooperative market architecture. Note that $W^{nc} \leq W^c$ and $W_a^{nc} \leq W_a^c$. This efficiency loss $W_a^c - W_a^{nc}$ is commonly known as the “price of anarchy” due to the strategic behavior of non-cooperative agents when payoff externalities exist.

We define *risk* to be the tail probability of the stationary process of aggregate demand:

$$R = \Pr(U(t) > M) \quad (2.9)$$

for some positive large constant M . As a result of marginal cost pricing and increasing marginal cost, risk also captures the tendency for aggregate demand / prices to spike drastically (above a large M). We also define *market robustness* to be:

$$B = 1 - R. \quad (2.10)$$

Apart from market efficiency, risk, in terms of demand spikes, is also an important welfare metric. In a given oligopolistic market, rational agents respond to endoge-

nous realtime prices to minimize individual costs. However, a system designer may have interests different from the agents, and be concerned about the risk, in particular the aggregate demand spikes or cost surges. In the sequel, we shall demonstrate, by analyzing the case with $L = 2$, that under the non-cooperative market architecture, even though there is a efficiency loss, the strategic behavior also results in a smaller tail probability, which is associated with a lower endogenous risk. A more fundamental question that we attempt to address is to what extent exogenous uncertainties is inevitable and to what extent it can be controlled in the system. More specifically, is there a limit of the feedback control, in the form of load scheduling, to achieve the dual goals of increasing market efficiency and reducing endogenous risk? Later we will show that for a broad class of load scheduling strategies, the exogenous randomness cannot be completely eliminated, and the dual goals cannot be achieved simultaneously.

So far, we have formulated the load scheduling problem as a stochastic dynamic oligopolistic game under the non-cooperative market architecture, and as an infinite horizon average cost MDP under the cooperative market architecture. In general, there are no closed form solutions to either of the two formulations, and numerical solutions involve exponential complexity. In the following chapter, we will look into the case where the number of types $L = 2$, and the equilibrium strategy as well as the optimal cooperative strategy can be found explicitly .

Chapter 3

Tradeoff Analysis for $L = 2$ Case

3.1. Equilibrium Strategy and Optimal Cooperative Strategy

When $L = 2$, there are only two types of agents in the system: type 1 agents with uncontrollable loads that must be satisfied upon arrival, and type 2 agents who have the flexibility to split the consumption between two consecutive time periods. Under the assumption of Bernoulli arrival process, at any time t , there are at most 3 agents in the market, which are indexed as: $(1, 1)_t$, $(2, 1)_t$, and $(2, 2)_t$. Among the three agents, only the type 2 agent $(2, 2)_t$ that arrives in the current period needs to make a nontrivial decision, while the other two agents have no choice but to empty their backlogs and leave the market.

Note that this simple case still retains the two key features of the general model. Firstly, since the active time window between any two consecutive type 2 agents partially overlap, when a type 2 agent schedules his consumption, he needs to take into account the action of the preceding type 2 agent, as well as to anticipate the

reaction of the succeeding type 2 agent, in a similar way of the sequential Stackelberg competition [16]; secondly, this dynamic system has exogenous uncertainties in terms of agent arrivals and load realizations. Considering the case of $L = 2$ sheds light on understanding agent behaviors induced by oligopolistic market architectures in the general setup. In electricity market, this case with a few oligopolistic agents can be used to study the interaction among a few load aggregators, each of which has considerable market power.

We first simplify the notations. When agent $(2, 2)_t$ schedules his consumption $(u_{(2,2)}(t), u_{(2,1)}(t))$, the sufficient statistics of system state for him is $(x(t), d_2(t))$, where $x(t) = x_{(1,1)}(t) + x_{(2,1)}(t)$ is defined as the *aggregate backlog* state. We also define a *linear strategy* as a strategy profile $\mathbf{u}(\mathbf{s})$ if $u_{(1,1)}(\mathbf{s}) = x_{(1,1)}$, $u_{(2,1)}(\mathbf{s}) = x_{(2,1)}$, and $u_{(2,2)}(\mathbf{s}) = u(x, d_2)$ which is a linear function of x and d_2 , i.e.,

$$u(x, d_2) = -ax + bd_2 + g.$$

Proposition 1 (Existence of linear MPE) *For $L = 2$, under the non-cooperative market architecture, there exists a Markov perfect symmetric equilibrium with the linear strategy $u^{nc}(x, d_2)$ given by:*

$$u^{nc}(x, d_2) = - \underbrace{\frac{1}{2(1 + \sqrt{1 - \frac{q_2}{2}})}}_{a^{nc}} x + \underbrace{\frac{1}{1 + \frac{1}{\sqrt{1 - \frac{q_2}{2}}}}}_{b^{nc}} d_2 + \underbrace{\frac{q_1\mu_1 + q_2\mu_2 \frac{1}{1 + \sqrt{1 - \frac{q_2}{2}}}}{2(1 + \sqrt{1 - \frac{q_2}{2}})}}_{g^{nc}} \quad (3.1)$$

Proof 1 *Please refer to Appendix C.1*

The optimal stationary cooperative strategy can also be obtained as a closed form solution of the Bellman equation with $L = 2$.

Proposition 2 (Existence of linear optimal stationary cooperative strategy)

For $L = 2$, under the cooperative market architecture, there exists a linear optimal stationary cooperative load scheduling strategy $u^c(x, d_2)$ given by:

$$u^c(x, d_2) = - \underbrace{\frac{1}{1 + \sqrt{1 - q_2}}}_{a^c} x + \underbrace{\frac{1}{1 + \frac{1}{\sqrt{1 - q_2}}}}_{b^c} d_2 + \underbrace{\frac{q_1 \mu_1 + q_2 \mu_2 \frac{1}{1 + \sqrt{1 - q_2}}}{1 + \sqrt{1 - q_2}}}_{g^c} \quad (3.2)$$

Proof 2 Please refer to Appendix C.2.

3.2. Welfare Impacts

Given a linear strategy $u(x, d_2) = -ax + bd_2 + g$, ($a \in (0, 1)$), we have the state evolution dynamics:

$$x(t + 1) = o_{(1,1)}(t + 1)d_1(t + 1) + o_{(2,2)}(t)(d_2(t) - u(x(t), d_2(t)))$$

which pins down the stationary distribution \mathcal{X} of the aggregate backlog state $\{x(t) : t \in \mathbb{Z}\}$ and \mathcal{U} of the aggregate demand process $\{U(t) : t \in \mathbb{Z}\}$, and it also determines the efficiency and risk performance.

Take expectation on both side of the aggregate backlog state dynamics, and we obtain the first and second moment of \mathcal{X} as follows:

$$\begin{aligned} \mathbb{E}[x(t)] &= \frac{q_1 \mu_1 + q_2((1 - b)\mu_2 - g)}{1 - q_2 a} \\ \mathbb{E}[x(t)^2] &= \frac{1}{1 - q_2 a^2} \left[q_1(\mu_1^2 + \sigma_1^2) + q_2 \left(((1 - b)\mu_2 - g)^2 + (1 - b)^2 \sigma_2^2 \right) + 2q_1 q_2 \mu_1 ((1 - b)\mu_2 - g) \right. \\ &\quad \left. + 2 \frac{a}{1 - q_2 a} \left(q_2((1 - b)\mu_2 - g) + q_1 q_2 \mu_1 \right) \left(q_2((1 - b)\mu_2 - g) + q_1 \mu_1 \right) \right] \end{aligned}$$

Assuming that all type 2 agents adopt the same linear strategy $u(x, d_2) = -ax + bd_2 + g$, market efficiency, as defined in (2.8), is given by:

$$\begin{aligned} W &= -\mathbb{E}[U(t)^2]/2 \\ &= -\frac{1}{2}\left((1 - q_2 + q_2(1 - a)^2)\mathbb{E}[x(t)^2] + 2q_2(1 - a)(b\mu_2 + g)\mathbb{E}[x(t)] + q_2((b\mu_2 + g)^2 + b^2\sigma_2^2)\right) \end{aligned}$$

In particular, with the specific linear strategies $u^{nc}(\cdot, \cdot)$ and $u^c(\cdot, \cdot)$, we can calculate the efficiency W^{nc} and W^c under the non-cooperative and the cooperative market architectures. The difference $\Delta = W^c - W^{nc}$ is positive and increasing in q_2 , as well as increasing in σ_1^2 and σ_2^2 , the variance of the workload distributions. The higher q_2 is, the larger efficiency loss of non-cooperative scheme will be, which suggests that the cooperative load scheduling scheme becomes increasingly efficient as the arrival rate of flexible loads increases.

However, the stationary distributions of the aggregate demand processes in Figure B-6 show that the cooperative scheme also thickens the right tail of the outcome distribution, which extremely high aggregate demands are quantified as a higher upper bound of risk in the following proposition.

Proposition 3 (Upper bound on the risk R) *Suppose that the workload distribution D_i are Normal distributions $\mathcal{N}(\mu_i, \sigma_i^2)$ for $i = 1, 2$. Given a linear strategy $u(x, d_2) = -ax + bd_2 + g$, ($a \in (0, 1)$), which leads to a stationary aggregate backlog distribution \mathcal{X} , the probability of aggregate backlog exceeding M is upper bounded by:*

$$\Pr(x(t) > M) \leq \frac{1}{\sqrt{2\pi}m_1} e^{-\frac{m_1^2}{2}}$$

where

$$m_1 = \frac{M - \frac{\mu_1 + (1-b)\mu_2 - g}{1-a}}{\sqrt{\frac{\sigma_1^2 + (1-b)^2\sigma_2^2}{1-a^2}}}.$$

Moreover, if the following condition is satisfied:

$$\frac{1 - (1-a)^2}{1-a^2} > \frac{b^2}{\frac{\sigma_1^2}{\sigma_2^2} + (1-b)^2} \quad (3.3)$$

the risk of aggregate backlog exceeding M is upper bounded as follows:

$$R = \Pr(U(t) > M) \leq q \Pr(x(t) \geq M) + o(e^{-M}) \text{ as } M \rightarrow \infty \quad (3.4)$$

Proof 3 Please refer to Appendix C.3.

Note that both $\mathbb{E}[x(t)]$ and $\mathbb{E}[x(t)^2]$ are increasing in a , and decreasing in b and g . It is easy to verify that the stationary distribution of $x(t)$ induced by the linear optimal cooperative strategy $u^c(\cdot, \cdot)$, has a larger mean and a larger variance than that induced by the non-cooperative equilibrium strategy $u^{nc}(\cdot, \cdot)$. In other words, the state of the aggregate backlog is more volatile in the cooperative scheme. Also, when $\sigma_1 = \sigma_2$, the cooperative market architecture leads to a higher upper bound of risk than that under the non-cooperative market architecture. This is consistent with the following simulation results where the cooperative scheme indeed results in a higher risk than that in the non-cooperative scheme. The interpretation of the condition in (3.3) is that, when the variance of flexible load realizations is sufficiently lower than that of the uncontrollable load realizations, and when the coefficient a is relatively large than the coefficient b , the aggregate demand spikes are mostly contributed by the high aggregate backlogs.

Remark 2 (Interpretation of the coefficients) For a linear strategy $u(x, d_2) =$

$-ax + bd_2 + g$ adopted by type 2 agents, the coefficient a can be interpreted as the sensitivity to the aggregate backlog $x(t)$. A larger a means that the strategy is more aggressive in absorbing the fluctuation of uncontrollable loads in the environment. Note that both a^{nc} and a^c are increasing in q_2 . Intuitively, with a higher type 2 arrival rate q_2 , each type 2 agent is more aggressive in responding to $x(t)$ at their first period, anticipating that during the second period will arrive and respond to $x(t+1)$ in a similar aggressive way. Also note that for any arrival rate q_2 , $a^{nc} < a^c$ always holds, and $a^c \in [0.5, 1]$, $a^{nc} \in [0.25, 0.2929]$, which means that type 2 agents always respond less aggressively to the aggregate backlog $x(t)$ under the non-cooperative market architecture. This can be understood as a result of their strategic behavior at equilibrium. Similarly, we can interpret the coefficient b as the sensitivity to the realizations of $d_2(t)$. We also make the observations that $b^{nc} > b^c$, and both b^{nc} , b^c are decreasing in q_2 .

3.3. Numerical results

In the following, we shall visualize the efficiency-risk tradeoffs. In particular, we compare the stationary distribution of the aggregate demand process induced by four different linear strategies. We have $u^c(\cdot, \cdot)$ from the cooperative scheme, and $u^{nc}(\cdot, \cdot)$ from the non-cooperative scheme. In addition, we define the “naive load scheduling” scheme to be $u^{naive}(x, d_2) = d_2/2$, in which case every type 2 agent evenly splits his work load between his two periods, and define the “no load scheduling” scheme to be $u^{no}(x, d_2) = d_2$, in which case every type 2 agent completes his work load at his first period.

- Figure B-3a shows the efficiency performance, which is negatively proportional to the second order moment of the aggregate demand process, under the four

strategies. We observe that as the arrival rate q_2 of type 2 agents increases, $\mathbb{E}[U(t)^2]$ increases for every strategy. This is mainly due to the increase in the workload. We also observe the efficiency loss of the non-cooperative load scheduling scheme when compared to the cooperative scheme for all arrival rates.

Figure B-3b shows the variance of the aggregate demand process as the arrival rate q_2 increases from 0 to 1. The variance is contributed by the uncertainties from both the Bernoulli arrival process and the workload realizations, and effective load scheduling tends to attenuate the variance. Since the uncertainty from the Bernoulli arrival process achieves its maximum at $q_2 = 1/2$, the variance versus the rate q_2 plots have the hump shape. Also, we observe that the variance gap between the non-cooperative and the cooperative scheme increases as q_2 increases. This indicates that the cooperative load scheduling becomes more powerful in terms of attenuating the aggregate demand variance when the arrival rate of flexible loads increases.

- Figure B-4 compares the risk of spikes across the four strategies. The 0.95-quantile of the stationary distribution of the aggregate demand process is plotted for each strategy. A higher 0.95-quantile is associated with a higher risk for some large constant M . The 0.95-quantile increases in q_2 mostly due to the heavier workload arrival. We also observe that as the arrival rate q_2 increases, risk increases most rapidly with the cooperative scheme, while the non-cooperative scheme gives the lowest risk for all q_2 and only slightly increases as the arrival rate increases.
- Figure B-5 shows the sample paths of the aggregate demand process under the non-cooperative and the cooperative market architecture. In Figure B-5a, we

observe that at a smaller time scale, the cooperative scheme can better smooth the aggregate demand process, which is consistent with the lower aggregate demand variance. However in Figure B-5b, at a larger time scale, we can identify more demand spikes produced endogenously by the cooperative load scheduling scheme, corresponding to the higher risk of the cooperative scheme.

- Figure B-6 plots the empirical distributions of the aggregate demand process in both linear scale in Figure B-6a and in log scale in Figure B-6b. We observe that under the cooperative market architecture, the distribution is more concentrated around the mean. However, associated with a higher risk, the distribution also has a heavier tail when compared to that in the non-cooperative scheme.

Figure B-12 shows the resulting aggregate demand stationary distribution of the cooperative and the non-cooperative load scheduling scheme under the non-negative demand constraint. We observe that it qualitatively resembles the corresponding distribution Figure B-6 in most essential aspects.

Remark 3 (When do spikes occur) *A better understanding the local interaction between agents with flexible loads also helps to discover the origin of endogenous risk, namely the triggers for demand spikes. On one hand, the instantaneous aggregate demand will be driven up when the workload realization $d_i(t)$ from either type of agent is extremely high, which corresponds to the rare events of the load arrival processes. We classify this type of spikes to be exogenous. Moreover, for bounded support of \mathbf{D}_i and large enough constant M , the exogenous shocks do not directly contribute to the risk measure. On the other hand, an aggregate spike can also be produced endogenously when there is a sudden absence of type 2 agent arrival after some consecutive periods during which type 2 agents continued to arrive, upon which*

event the accumulated high aggregate backlog at the deadline translates into a demand spike.

When obtaining the risk upper bound in Proposition 3, we made use of the fact that most of the spikes are produced endogenously. This observation is further confirmed by the conditional distributions of aggregate demand process in Figure B-7. We can see that the tail of the aggregate demand distribution is much larger conditional on that there is no type 2 agent arrival, and is much larger conditional on that the aggregate backlog is high. Intuitively, the more efficient a load scheduling strategy is, the more intense the backlog usage will be, and the resulting high backlog volatility leads to demand spikes.

We also point out that the tradeoffs we observed hold not only between the cooperative and non-cooperative market architectures above, but also exist in a variety of oligopolistic market architectures. Even when the agents can coordinate their actions and are risk sensitive, so that large spikes are mitigated, the tradeoff still exists and is shaped by different market architectural properties. In Appendix D.1, we provide two parameterized variations of the market architectures, where the number of new arrival of each type can be great than 1, and where the agents can be risk sensitive, separately.

Chapter 4

General L Analysis: Pricing

As illustrated in Figure B-2a, the agents who make their load scheduling decisions can be viewed as a full state feedback controller, the control signal $\mathbf{u}(t)$ is fed back to the plant and affects the system state evolution according to (2.3) and (2.4), and the system output is the aggregate demand process $\{U(t) : t \in \mathbb{Z}\}$. In the case with $L = 2$, even when the existing agents adopt a linear strategy, the system dynamics is not linear since the type 2 agents $(2, 2)_t$ do not arrive at every period t . For a general L , the load scheduling strategy, which is determined under a specific market architecture, does not form a linear time-invariant feedback controller. The non-linearity as a result of the Bernoulli arrival processes complicates the analysis, and there is no explicit solution to the equilibrium load scheduling strategy under marginal cost pricing in both the cooperative and the non-cooperative schemes.

We realize that the main hurdle of analyzing the general L case lies in the non-linear dynamics due to the intermittent agent arrivals. To circumvent the problem we shall introduce a modified system with surrogate performance measures, which resembles the original system in the most essential ways and facilitates the analy-

sis. The results obtained in this LTI framework provide us some insights on the original non-linear system dynamics and the efficiency-risk tradeoffs. The two key modifications are listed and interpreted as follows:

Modification 1 *The agent arrival rate $\mathbf{q} = \mathbf{1}$, namely agents of all types arrive at every period, so that $\mathbf{h}(t) = \mathbf{1}$ and $\mathbf{o}(t) = \mathbf{1}$ for all t .*

Modification 2 *The second moment $\mathbb{E}[z_2(t)^2]$ of the aggregate backlog process $z_2(t) = \mathbf{e}'\mathbf{x}(t)$ is used as a substitute measure for risk.*

Observations of the correlation between spikes and backlog, as well as the correlation between spikes and the absence of flexible loads in Remark 3 motivate us to use the backlog volatility as a substitute measure for the risk. Notice that there is no contradiction between the first two modifications. We examine the case with $\mathbf{q} = \mathbf{1}$, and the equilibrium strategy, as well as the evolution of the backlog state in the regime of high arrival rate \mathbf{q} will be similar to the case of $\mathbf{q} = \mathbf{1}$; however, absence of flexible loads still happens exogenously with small probabilities, and upon which occurrences a high backlog is turned into a demand spike. Therefore, the volatility of the aggregate backlog state is used as a substitute measure for the risk of spikes.

We also normalize the load arrival process so that the average load realization $\boldsymbol{\mu}$, the average backlog state $\mathbb{E}[\mathbf{x}(t)]$, and the average demand $\mathbb{E}[\mathbf{u}(t)]$, are all zero vectors. We also assume the load arrival process $\{\mathbf{d}(t) : t \in \mathbb{Z}\}$ is an i.i.d. process. In summary, the system diagram of the modified system with linear dynamics is shown in Figure B-2b. The performance measures are the variance of the two outputs:

$$\begin{bmatrix} z_1(t) \\ z_2(t) \end{bmatrix} = \begin{bmatrix} \mathbf{e}'\mathbf{u}(t) \\ \mathbf{e}'\mathbf{x}(t) \end{bmatrix}.$$

From the system operator’s view, we are interested in how agent decision making is shaped by the market architecture, and how the architecture should be designed so that the desired agent behavior is induced. Usually many of the market architectural properties, for example the degree of cooperation and risk sensitivity of the agents, are given, and the system operator’s only freedom is to design the pricing rule. In the following, we shall consider a non-cooperative setup within the LTI framework, and examine the equilibrium load scheduling strategies under any linear pricing rule, which will be decided by the system operator¹. In particular, we focus on the static linear pricing rules parameterized by coefficients \mathbf{q}_1 and \mathbf{q}_2 , in the form:

$$p(t) = \mathbf{q}'_1 \mathbf{x}(t) + \mathbf{q}'_2 \mathbf{u}(t). \quad (4.1)$$

The instantaneous demand decisions are made by individual agents under the deadline constraints in a non-cooperative way. We restrict ourselves to the linear symmetric MPE, assuming that the load scheduling strategy, if exists, is in the following form:

$$\mathbf{u}^*(t) = \mathbf{F}^* \mathbf{x}(t), \quad (4.2)$$

and we denote the (l, τ) -th row of \mathbf{F}^* by $\mathbf{F}^*_{(l,\tau)} \in \mathbb{R}^{D_c}$. By individual rationality, $u_{(l,\tau)}(t)$ is optimized by agent $(l, \tau)_t$ when he dynamically updates his load scheduling decision, forming the rational expectation that all other agents are adopting the equilibrium linear strategy as in (4.2). More specifically, apply the one-shot deviation principle at the equilibrium and we have the optimal load scheduling decision $u^*_{(l,\tau)}(t)$

¹ In Appendix D.3, we study another example where the system operator regulates the architectural property of “degree of cooperation” by imposing a “congestion fee”, which in effect works to internalize the payoff externalities.

given by:

$$\forall (l, \tau) \in \mathcal{C}, \text{ if } \tau > 1, \quad u_{(l, \tau)}^*(t) = \arg \min_{u \in \mathbb{R}} \left\{ \mathbf{p}(t)u + \mathbb{E} \left[\sum_{k=1}^{\tau-1} \mathbf{p}(t+k) \mathbf{F}_{(l, \tau-k)}^* \mathbf{x}(t+k) \right] \right\} \quad (4.3)$$

$$\text{subject to: } \mathbf{u}(t) = \mathbf{F}^* \mathbf{x}(t) + \mathbf{e}_{(l, \tau)}(u - \mathbf{F}_{(l, \tau)}^* \mathbf{x}(t))$$

$$\mathbf{u}(t+k) = \mathbf{F}^* \mathbf{x}(t+k), \quad \forall k > 0$$

$$p(i) = \mathbf{q}'_1 \mathbf{x}(i) + \mathbf{q}'_2 \mathbf{u}(i), \quad \forall i$$

$$\mathbf{x}(i+1) = \mathbf{R}_1 \mathbf{x}(i) + \mathbf{R}_2 \mathbf{d}(i) - \mathbf{R}_1 \mathbf{u}(i), \quad \forall i$$

$$\text{if } \tau = 1, \quad u_{(l, \tau)}^*(t) = \mathbf{e}_{(l, \tau)} \mathbf{x}(t),$$

where $\mathbf{e}_{(l, \tau)}$ is a D_c dimensional vector with the only non-zero element being 1 at the (l, τ) -th position. Moreover, at the symmetric equilibrium the rational expectation should be consistent with the best response strategy, namely (4.2) should be satisfied.

A direct application of the principle of optimality to (4.3) leads to

$$\mathbf{F}^* = f_{(\mathbf{q}_1, \mathbf{q}_2)}(\mathbf{F}^*). \quad (4.4)$$

For given coefficients $\mathbf{q}_1, \mathbf{q}_2$, the (l, τ) -th row of the mapping $f_{(\mathbf{q}_1, \mathbf{q}_2)} : \mathbb{R}^{D_c \times D_c} \rightarrow \mathbb{R}^{D_c \times D_c}$ is specified as follows:

$$f_{(\mathbf{q}_1, \mathbf{q}_2)}(\mathbf{F})_{(l, \tau)} = \begin{cases} \mathbf{e}'_{(l, \tau)} & \text{if } \tau = 1, \\ \frac{\mathbf{e}'_{(l, \tau)} \mathbf{R}'_1 \mathbf{A}_{(l, \tau)} \left(\mathbf{R}_1 (\mathbf{I} - \mathbf{F}) + \mathbf{R}_1 \mathbf{e}_{(l, \tau)} \mathbf{F}_{(l, \tau)} \right) - \left(\mathbf{q}'_1 + \mathbf{q}'_2 (\mathbf{F} - \mathbf{e}_{(l, \tau)} \mathbf{F}_{(l, \tau)}) \right)}{\mathbf{e}'_{(l, \tau)} \mathbf{R}'_1 \mathbf{A}_{(l, \tau)} \mathbf{R}_1 \mathbf{e}_{(l, \tau)} + 2\mathbf{e}'_{(l, \tau)} \mathbf{q}_2} & \text{if } \tau > 1, \end{cases} \quad (4.5)$$

where

$$\mathbf{A}_{(l,\tau)} = \sum_{k=1}^{\tau-1} \left((\mathbf{R}_1(\mathbf{I}-\mathbf{F}))^{k-1} \right)' \left((\mathbf{q}_1 + \mathbf{F}'\mathbf{q}_2)\mathbf{F}_{(l,\tau-k)} + \mathbf{F}'_{(l,\tau-k)}(\mathbf{q}'_1 + \mathbf{q}'_2\mathbf{F}) \right) \left((\mathbf{R}_1(\mathbf{I}-\mathbf{F}))^{k-1} \right).$$

The highly nonlinear mapping $f_{(\mathbf{q}_1, \mathbf{q}_2)}$ is not a contraction, and obtaining the conditions on the parameters which guarantee the existence of a fixed point solution to (4.5) is a challenging task. However, the equation still provides a set of necessary conditions for the equilibrium strategies to satisfy. An iteration algorithm with a carefully chosen initial guess will converge to such a fixed point, and we will use numerical examples to show how the pricing parameter \mathbf{q}_1 and \mathbf{q}_2 shift the equilibrium.

Proposition 4 (System operator's problem) *Assume the system operator's utility function is increasing in efficiency and decreasing in risk, and in particular is linearly decreasing in both the volatility of aggregate demand and aggregate backlog as follows:*

$$J(\mathbb{E}[z_1(t)^2], \mathbb{E}[z_2(t)^2]) = -(\alpha_1 \mathbb{E}[z_1(t)^2] + \alpha_2 \mathbb{E}[z_2(t)^2]).$$

The system operator optimizes the parameterized pricing rule as defined in (4.1) to maximize its utility, and the optimal solution $(\mathbf{q}_1^, \mathbf{q}_2^*)$ is given by solving the following problem:*

$$\min_{\mathbf{q}_1, \mathbf{q}_2 \in \mathbb{R}^{D_c}, \mathbf{Q}, \mathbf{F} \in \mathbb{R}^{D_c \times D_c}} \alpha_1 \mathbf{e}' \mathbf{F}_{(\mathbf{q}_1, \mathbf{q}_2)} \mathbf{Q} \mathbf{F}_{(\mathbf{q}_1, \mathbf{q}_2)} \mathbf{e} + \alpha_2 \mathbf{e}' \mathbf{Q} \mathbf{e} \quad (4.6)$$

$$\text{subject to: } \mathbf{R}_1(\mathbf{I} - \mathbf{F})\mathbf{Q}(\mathbf{I} - \mathbf{F}')\mathbf{R}'_1 - \mathbf{Q} + \mathbf{R}_2\mathbf{R}'_2 = \mathbf{0} \quad (4.7)$$

$$\mathbf{F} = f_{(\mathbf{q}_1, \mathbf{q}_2)}(\mathbf{F}) \quad (4.8)$$

where $f_{(\mathbf{q}_1, \mathbf{q}_2)}$ is the mapping defined in (4.5).

Proof 4 Please refer to Appendix C.4.

Chapter 5

General L Analysis: fundamental tradeoff

In Chapter 4, we have introduced the modified system, as well as evaluated the MPE strategy and system performance in a non-cooperative setup under linear pricing rules. The following interesting questions naturally arise: are the equilibrium load scheduling strategies in the non-cooperative setup optimal? If not, given the system dynamics what are the optimal strategies? Does there exist a market architecture that induces such optimal strategies? This chapter is devoted to an examination of these questions.

Ideally, the desirable load scheduling should simultaneously maximize efficiency and minimize risk, or equivalently in the modified setup, simultaneously suppress the volatility of the two measured processes: $z_1(t)$ and $z_2(t)$. A load scheduling strategy is defined to be Pareto optimal if there does not exist any other strategy that makes the volatility of $z_1(t)$ smaller without making the volatility of $z_2(t)$ larger, and a pair $(\mathbb{E}[z_1(t)^2], \mathbb{E}[z_2(t)^2])$ locates on the Pareto front if it is achieved by a

Pareto optimal strategy. Unless the Pareto front trivially includes the point $(0, 0)$, it dictates the limit of the system performances with a downward sloping tradeoff curve between efficiency and risk. Also note that the concept of Pareto optimal load scheduling strategy does not rely on market architecture specifications, in the sense that the system performance achievable under any specific market architecture will be bounded by the Pareto front. The Pareto front thus serves as a benchmark to measure how far away a load scheduling strategy induced by a specific market architecture is from the optimal strategies.

In order to neatly characterize the set of Pareto optimal load scheduling strategies, we hereby introduce the third modification to the LTI system:

Modification 3 *The deadline constraints, which require that all agents empty their backlogged load when they exit the market, are relaxed. Instead, we track the total load mismatch upon their deadline:*

$$z_3(t) = \mathbf{e}'_L(\mathbf{x}(t) - \mathbf{u}(t)),$$

where \mathbf{e}_L is a D_c -dimensional column vector with the first L elements being ones and all others zero. We define the second moment $\mathbb{E}[z_3(t)^2]$ as the third performance measure. Note that the smaller the variance is, on average the more closely that deadline constraints are met, and when $\mathbb{E}[z_3(t)^2] = 0$, the deadline constraints are enforced.

Finally, after the three modifications, the system diagram with the inputs of load arrival processes and the outputs $\mathbf{z}(t) = [z_1(t), z_2(t), z_3(t)]$ is shown in Figure B-2c. We generalize the tradeoff between efficiency and risk to a three-way tradeoff among efficiency, risk, and load mismatch upon deadline, with the three-way Pareto optimal

strategies and the three-way Pareto front (a surface in the 3-dimensional space) similarly defined. Now we are able to cast the problem of finding Pareto optimal load scheduling strategy into a \mathcal{H}_2 optimization problem with an unconstrained feedback controller, which admits a convex characterization.

In order to trace out the Pareto front, we follow the standard multi-objective optimization technique to scalarize the objective. Consider the weighted output process:

$$\mathbf{z}_\alpha(t) = [\alpha_1 z_1(t), \alpha_2 z_2(t), \alpha_3 z_3(t)],$$

where $\alpha_i > 0$, for $i = 1, 2, 3$, and $\alpha_1^2 + \alpha_2^2 + \alpha_3^2 = 1$. A Pareto optimal load scheduling strategies minimize the \mathcal{H}_2 system norm for a given weight $\alpha = (\alpha_1, \alpha_2, \alpha_3)$:

$$\begin{aligned} & \min_{\{\mathbf{u}(t): t \in \mathbb{Z}\}} \|\mathbf{z}_\alpha(t)\|_2^2 \\ & \text{subject to: } \mathbf{x}(t+1) = \mathbf{R}_1(\mathbf{x}(t) - \mathbf{u}(t)) + \mathbf{R}_2 \mathbf{d}(t) \end{aligned}$$

Proposition 5 (Three-way Pareto front) 1. For given non-negative weight $\alpha = (\alpha_1, \alpha_2, \alpha_3)$, the corresponding Pareto optimal load scheduling strategy is static and linear in the system state $\mathbf{x}(t)$ as follows:

$$\mathbf{u}(t) = \mathbf{F}_\alpha^* \mathbf{x}(t).$$

where $\mathbf{F}_\alpha^* = \mathbf{Q}^* \mathbf{P}^{*-1}$, and $(\mathbf{Q}^*, \mathbf{P}^*)$ is the unique solution to the following convex

optimization problem:

$$\begin{aligned}
& \min_{\mathbf{Q}, \mathbf{P} \in \mathbb{R}^{D_c \times D_c}, \mathbf{M} \in \mathbb{R}^{3 \times 3}} \rho \\
\text{subject to: } & \mathbf{Q} > \mathbf{0}, \\
& \text{Trace}(\mathbf{M}) \leq \rho, \\
& \begin{bmatrix} \mathbf{Q} & (\mathbf{R}_1 \mathbf{Q} - \mathbf{R}_1 \mathbf{P})' \\ (\mathbf{R}_1 \mathbf{Q} - \mathbf{R}_1 \mathbf{P}) & \mathbf{Q} - \mathbf{R}_2 \mathbf{R}_2' \end{bmatrix} > \mathbf{0}, \\
& \begin{bmatrix} \mathbf{Q} & (\mathbf{C}_1 \mathbf{Q} + \mathbf{D}_{12} \mathbf{P})' \\ (\mathbf{C}_1 \mathbf{Q} + \mathbf{D}_{12} \mathbf{P}) & \mathbf{M} \end{bmatrix} > \mathbf{0}.
\end{aligned}$$

where

$$\mathbf{C}_1 = [0 \quad \alpha_2 \mathbf{e} \quad \alpha_3 \mathbf{e}_L]', \quad \mathbf{D}_{12} = [\alpha_1 \mathbf{e} \quad \mathbf{0} \quad -\alpha_3 \mathbf{e}_L]'$$

2. Given a matrix \mathbf{F} such that the feedback rule $\mathbf{u}(t) = \mathbf{F}\mathbf{x}(t)$ stabilizes the system, the \mathcal{H}_2 norm of the three performance measures is given by:

$$\|z_1(t)\|_2^2 = \mathbf{e}' \mathbf{F} \mathbf{Q}_F \mathbf{F}' \mathbf{e}; \quad \|z_2(t)\|_2^2 = \mathbf{e}' \mathbf{Q}_F \mathbf{e}; \quad \|z_3(t)\|_2^2 = (\mathbf{e}' - \mathbf{e}'_L \mathbf{F}) \mathbf{Q}_F (\mathbf{e}' - \mathbf{e}'_L \mathbf{F})'$$

where \mathbf{Q}_F is the controllability Gramian given by solving the following equation:

$$\mathbf{R}_1 (\mathbf{I} - \mathbf{F}) \mathbf{Q}_F (\mathbf{I} - \mathbf{F}') \mathbf{R}_1' - \mathbf{Q}_F + \mathbf{R}_2 \mathbf{R}_2' = \mathbf{0}$$

Proof 5 Please refer to Appendix C.5.

With different parameters of $\alpha = (\alpha_1, \alpha_2, \alpha_3)$, different Pareto optimal solutions are produced, and we can trace out the Pareto front. In particular, the curve when restricting the three-way Parato front to the plane of $\|z_3(t)\|_2^2 = \epsilon$ for $\epsilon \ll 1$ approaches

the efficiency-risk tradeoff curve when the deadline constraints are enforced, and the corresponding weight α satisfies $\alpha_3/\alpha_1 \gg 1$ and $\alpha_3/\alpha_2 \gg 1$.

As an example, in Figure B-8, we plot the Pareto front for the case with $L = 5$ to visualize the three-way tradeoff among the three system performance measures. In Figure B-9, we observe that as we tighten the constraint on load mismatch upon deadline, namely with a smaller β_3 in the constraint $\|z_3(t)\|_2^2 \leq \beta_3$, the two-way Pareto front of efficiency and risk shifts outward, which means that volatility of both aggregate demand and aggregate backlog will increase. Similarly, as the constraint on the second performance measure becomes tighter, namely with a smaller β_2 in the constraint $\|z_2(t)\|_2^2 \leq \beta_2$, the Pareto front of the other two measures shifts outward.

The second part of Proposition 5 provides a way to evaluate the system performance for any linear load scheduling strategies. In Appendix D.2, we introduce some parameterized classes of heuristic load scheduling strategies, the parameters of which reflect the market architectural properties. Numerical results reveal how the tradeoffs among the three goals are shaped, as well as how far they are away from the benchmark of the Pareto front characterized above.

Chapter 6

Conclusion

In this paper, we proposed a framework to examine the welfare impacts of load scheduling under different market architectures. We took the approach of modeling agent behavior with dynamic oligopolistic games, and pointed out that different market architectures induce different agent behaviors, which lead to a tradeoff between efficiency and risk at the aggregate level. Moreover, we provided a characterization of the efficiency-risk Pareto front. This is the fundamental tradeoff limit for the system with load scheduling dynamics, in the sense that the system performance induced by any market architecture is bounded by the front.

There are two directions of our future research. First, we would like to relax the complete information assumption, and examine the model with a large number of coexisting agents. This is the case in many real life applications including future electricity market, where small entities that own generation powers are able to participate, and system state is not globally available. Mean field game theory is a promising tool in analyzing agent behavior in this dynamic stochastic game with a large number of players. The interesting questions we want to address are: how do

agents react to local and systemic dynamics, and how is agent behavior shaped by the information structure? Moreover, when in the limit the market becomes competitive, does similar efficiency-risk tradeoff exist?

Secondly, we would like to look into the system operator's problem of optimizing the pricing rule. In our current work, the system performance is determined by the aggregation of autonomous agents's behavior, which relies on the pricing mechanism in an intricate way, and there is no tractable way for the system operator to design the pricing rule to induce the desired agent behavior. We are still exploring different formulations which can give us some insights on the problem of pricing mechanism design. More generally, realtime prices can be viewed as an endogenously generated payoff relevant signal sent by the system operator to the agents, aiming to induce the rational agents to respond to the signal in a desirable way. Another interesting question to ask is: what are the signaling schemes in general that can incentivize the agents to behave in certain ways?

Appendix A

Tables

$l \in \mathcal{L}$	agent type
$(l, \tau)_t \in \mathcal{C}$	at time t , the type l agent who will continue to stay in the market for τ periods
$\mathbf{d}(t) \in \mathbb{R}^L$	new agent load realization at time t
$\mathbf{h}(t) \in \{0, 1\}^L$	new agent arrival event at time t
$\mathbf{x}(t) \in \mathbb{R}^{D_c}$	backlog state
$\mathbf{o}(t) \in \{0, 1\}^{D_c}$	existence state
$\mathbf{s}(t) \in \mathcal{S}$	system state, $\mathbf{s}(t) = (\mathbf{x}(t), \mathbf{z}(t))$
$\mathbf{u}(t) \in \mathbb{R}^{D_c}$	instantaneous demand
$p(t)$	realtime price per unit resource
$U(t)$	instantaneous aggregate demand
\mathbf{u}^{nc}	symmetric Markov Perfect Equilibrium (MPE) load scheduling strategy
\mathbf{u}^c	optimal stationary cooperative load scheduling strategy
W	efficiency
R	risk
B	robustness

Table A.1: Notations

Appendix B

Figures

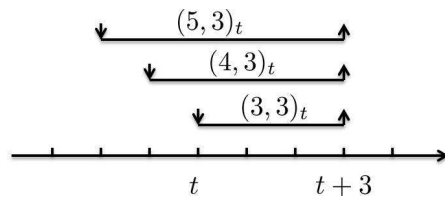
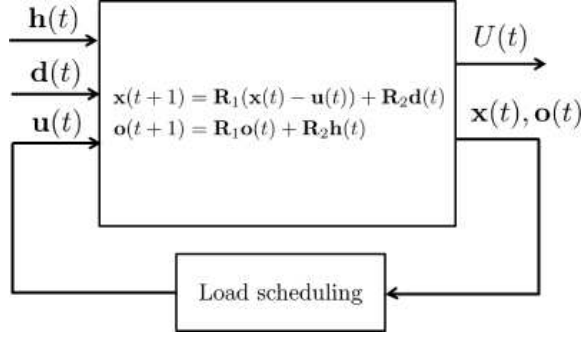
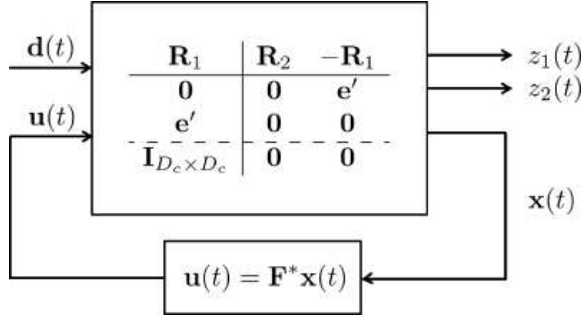


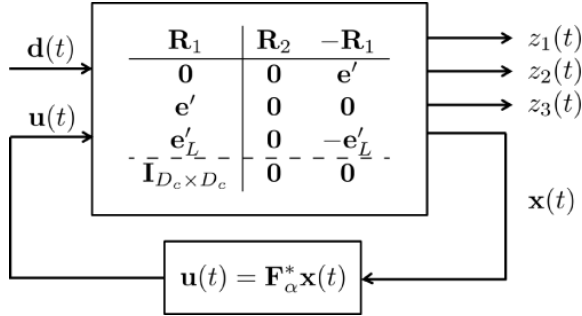
Figure B-1: Visualization of agent index $(l, \tau)_t$. For $L = 5$, $\tau = 3$, at time t there are at most 3 agents that will stay in the market for 3 periods. If they indeed arrive at the market, namely $h_3(t) = h_4(t - 1) = h_5(t - 2) = 1$, at time t they are indexed as $(5, 3)_t$, $(4, 3)_t$ and $(3, 3)_t$, separately.



(a) Original system dynamics with non-linear feedback controller.

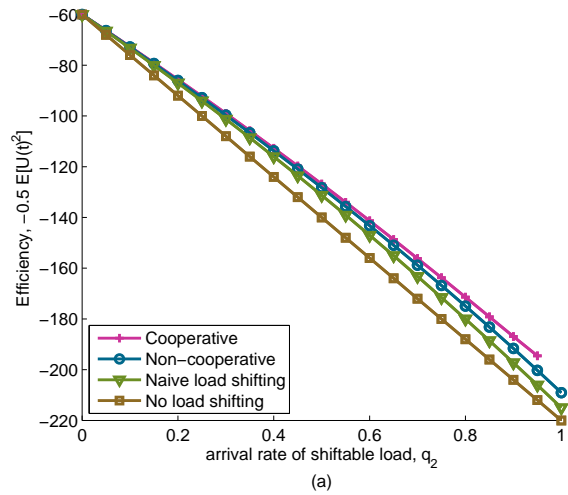


(b) Linear time-invariant system formulation. There are two measurements: aggregate output process $z_1(t)$, and aggregate backlog process $z_2(t)$. At equilibrium, load scheduling strategies of individual agents form a linear state feedback controller.

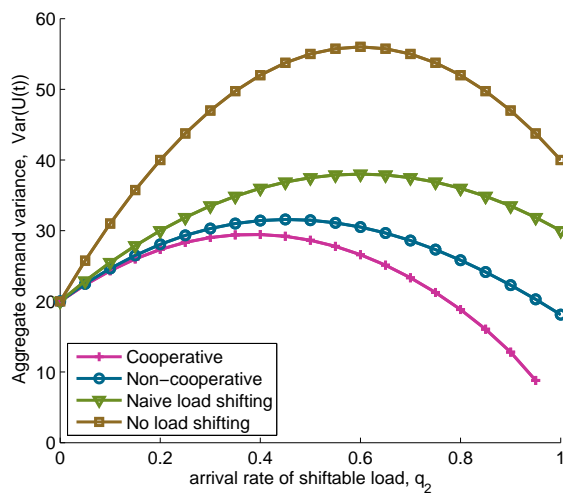


(c) Linear time-invariant system formulation with relaxed deadline constraint. There are three measurements: aggregate output process $z_1(t)$, aggregate backlog process $z_2(t)$, and aggregate load mismatch upon deadline $z_3(t)$. $\mathbf{u}(t) = \mathbf{F}^*_\alpha \mathbf{x}(t)$ is a Pareto optimal load scheduling strategy profile.

Figure B-2: System diagrams



(a)



(b)

Figure B-3: Market efficiency under different load scheduling schemes. System parameters as follows: the number of agent types $L = 2$; uncontrollable load Bernoulli arrival rate $q_1 = 1$; mean and variance of arrival load distribution $\mu_1 = \mu_2 = 10$, $\sigma_1 = \sigma_2 = 11$. The cooperative load scheduling scheme leads to a lower aggregate consumption variance and thus a higher efficiency than that of the non-cooperative load scheduling scheme. This is known as the “price of anarchy” of strategic behavior in non-cooperative game.

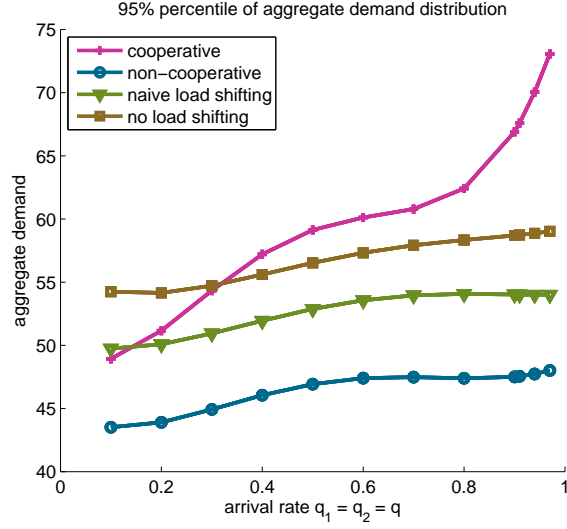
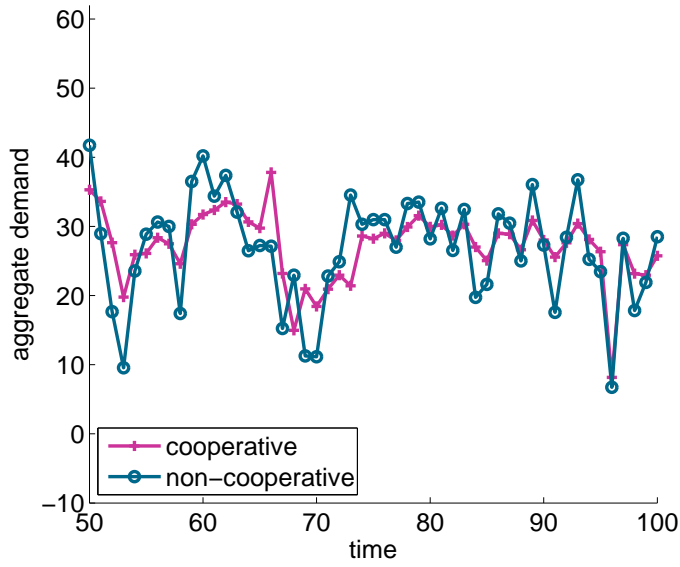
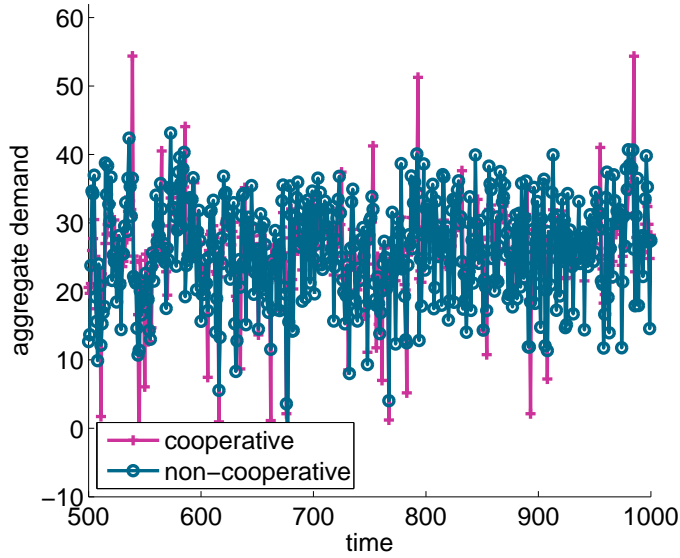


Figure B-4: Risk under different load scheduling schemes. For any arrival rate q , the stationary distribution of the aggregate demand process has a larger tail under the cooperative market architecture than that under the non-cooperative market architecture. System parameters as follows: the number of agent types $L = 2$; Bernoulli arrival rate $q_1 = q_2 = q$; mean and variance of arrival load distribution $\mu_1 = \mu_2 = 15$, $\sigma_1 = \sigma_2 = 4$.

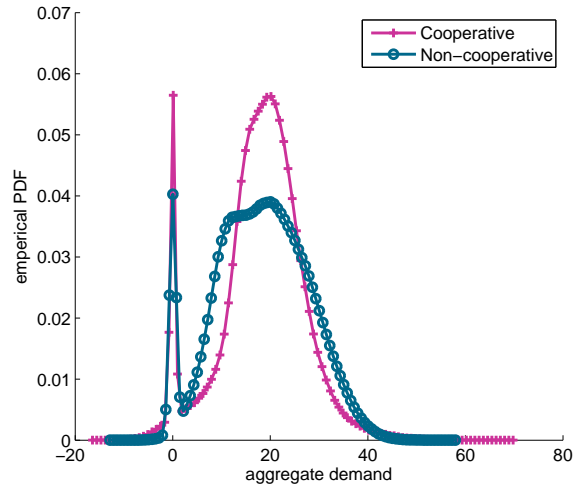


(a) Short time scale

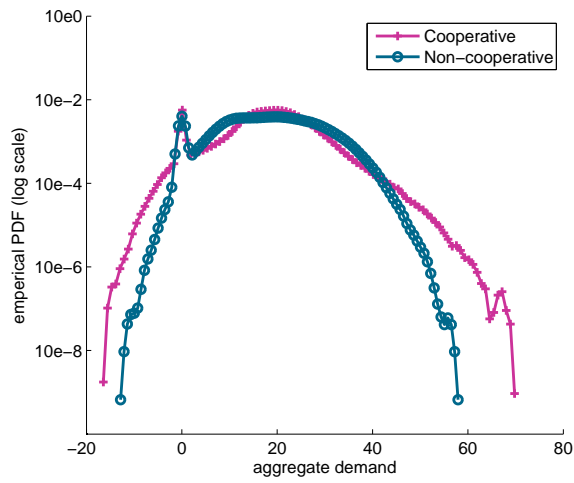


(b) Large time scale

Figure B-5: Sample paths of the aggregate demand process under the cooperative and the noncooperative load scheduling schemes. At a smaller time scale, the cooperative load scheduling can better smooth out the aggregate demand process. However, at a larger time scale, there are more demand spikes produced endogenously by the cooperative load scheduling scheme. This is consistent with the observation of “low variance, high tail probability” of aggregate demand stationary distribution under the cooperative market architecture. System parameters as follows: the number of agent types $L = 2$; Bernoulli arrival rate $q_1 = q_2 = 0.9$; mean and variance of arrival load distribution $\mu_1 = \mu_2 = 15$, $\sigma_1 = \sigma_2 = 6$.

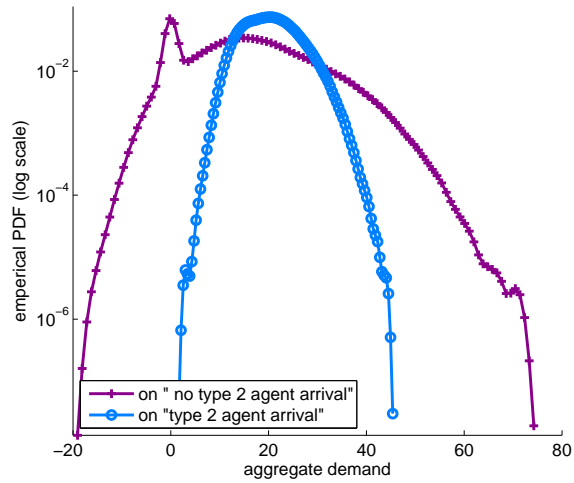


(a) PDF

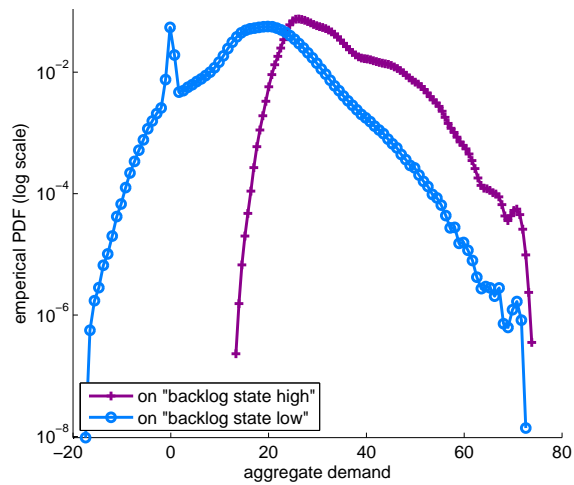


(b) PDF (in log scale)

Figure B-6: Empirical distribution of the stationary aggregate demand process under the cooperative and the noncooperative load scheduling schemes. The stationary distribution under the non-cooperative market architecture is more spread out but also has a smaller tail probability, while the distribution under the cooperative market architecture is more concentrated around the mean but also has a larger tail probability. System parameters as follows: the number of agent types $L = 2$; Bernoulli arrival rate $q_1 = q_2 = 0.6$; mean and variance of arrival load distribution $\mu_1 = \mu_2 = 15$, $\sigma_1 = \sigma_2 = 6$.



(a) Aggregate demand distribution (log scale) conditional on whether flexible loads arrive or not



(b) Aggregate demand distribution (log scale) conditional on whether aggregate backlog state is high or low

Figure B-7: Observations of when spikes happen. The extremely high aggregate demand (demand spikes) happen mostly when the flexible loads are absent and when the aggregate backlog state is high. Here we have $L = 2$, $\mathbf{D} \sim \mathcal{N}(0, \mathbf{I})$.

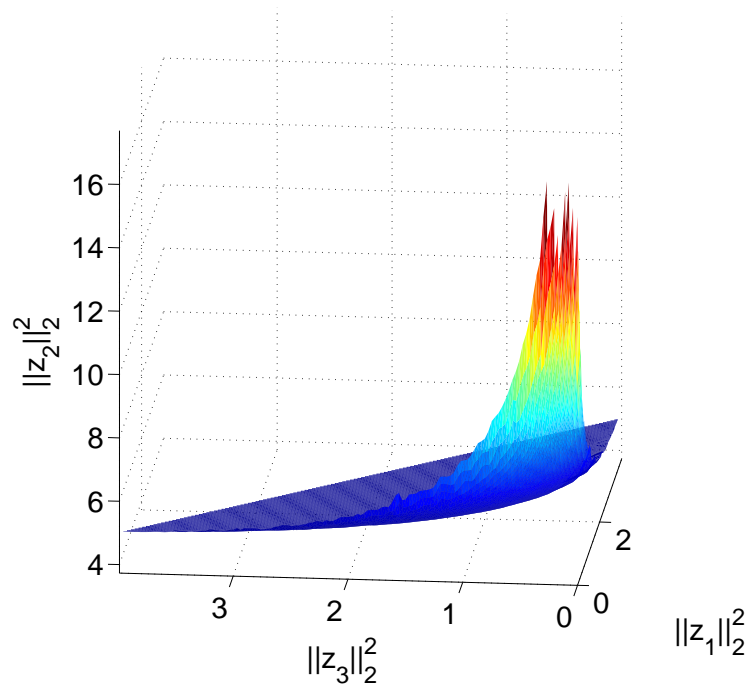
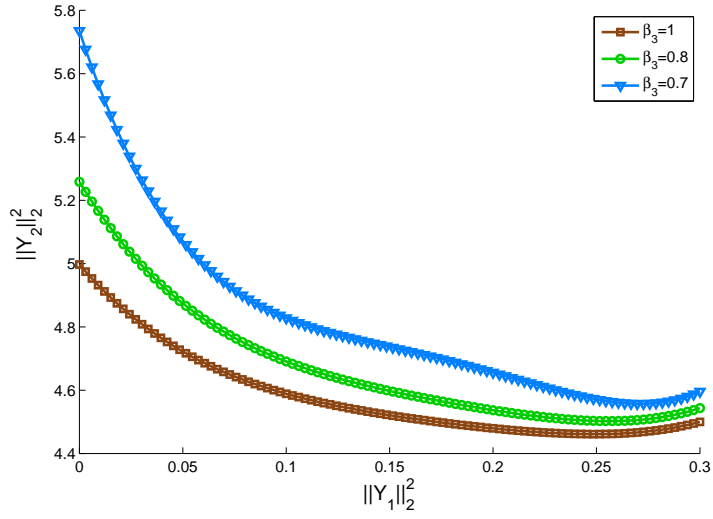
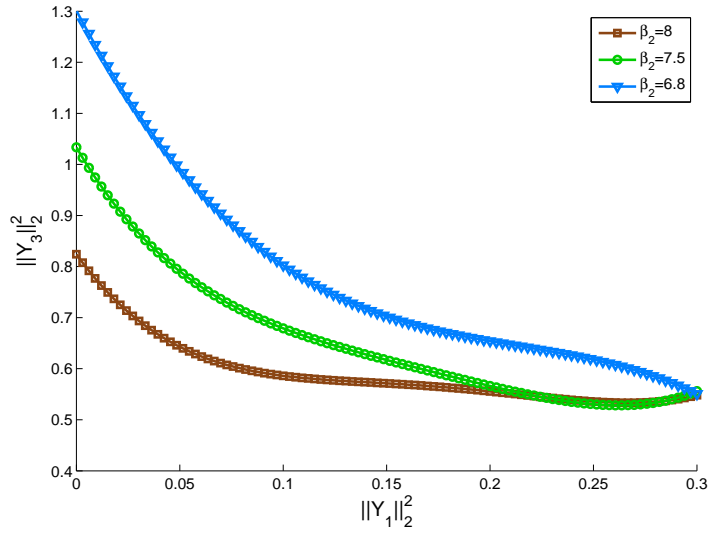


Figure B-8: The three-way Pareto front. The three objectives are $\|z_1\|_2^2$, $\|z_2\|_2^2$, and $\|z_3\|_2^2$, which are the variance of the aggregate demand, the aggregate backlog, and the aggregate load mismatch upon deadline, correspondingly. Parameters: $L = 5$.

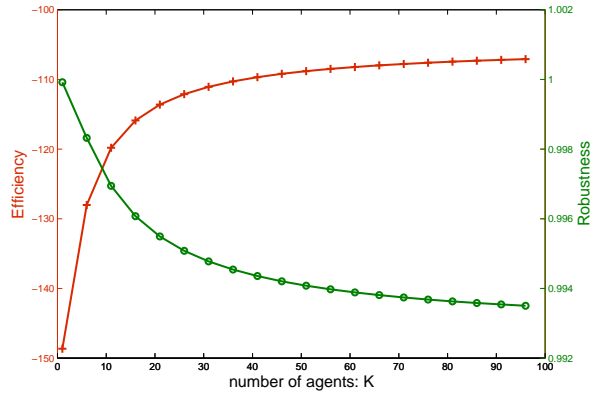


(a) When the constraint $\|z_3\|_2^2 \leq \beta_3$ is tightened, namely β_3 decreases, the Pareto front of $\|z_1\|_2^2$ and $\|z_2\|_2^2$ shifts outward.

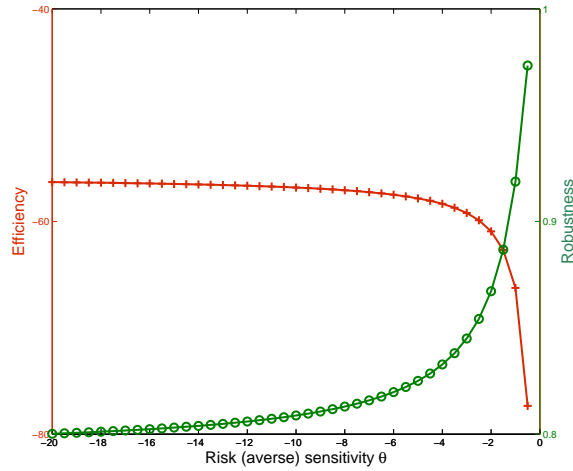


(b) When the constraint on $\|z_2\|_2^2 \leq \beta_2$ is tightened, namely β_2 decreases, the Pareto front of $\|z_1\|_2^2$ and $\|z_3\|_2^2$ shifts outward.

Figure B-9: Visualization of the three-way tradeoff Pareto front. The constraint on one performance measure affects the location of the tradeoff curve of the other two measures. Parameters: $L = 5$.



(a) Market power leads to efficiency-risk tradeoff. As the number of agents K increases, individual's market power decreases, efficiency increases at the cost of robustness.



(b) Risk sensitivity leads to efficiency-risk tradeoff. In the cooperative setup, as the magnitude of risk sensitivity $|\theta|$ increases, agent become more risk averse, and risk of spikes decreases. We observe a increase of robustness at the cost of a lower efficiency.

Figure B-10: Efficiency-risk tradeoffs as a result of different market architectural properties, in the case with $L = 2$.

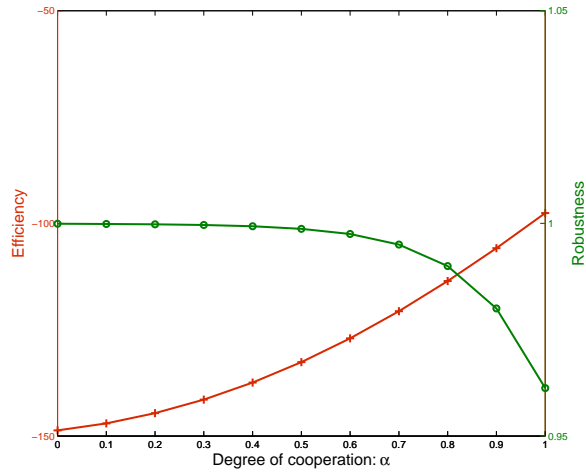
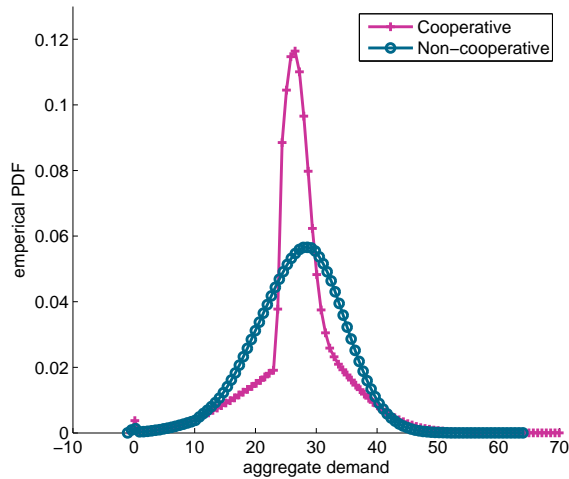
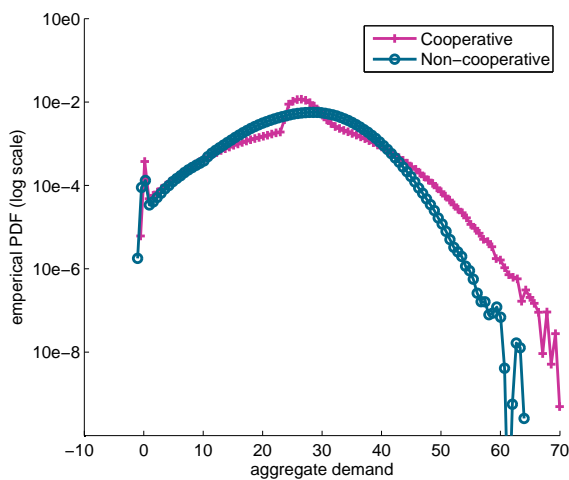


Figure B-11: Degree of cooperation leads to efficiency-risk tradeoff. As the system operator increases the “congestion fee” by increasing α , the payoff externality is reduced, and the degree of cooperation increases, leading to a higher efficiency and lower level of robustness.



(a) PDF



(b) PDF (in log scale)

Figure B-12: Empirical distribution of the stationary aggregate demand process under the constraint that the instantaneous demand from any agent is restricted to be non-negative. System parameters as follows: the number of agent types $L = 2$; Bernoulli arrival rate $q_1 = q_2 = 0.6$; mean and variance of arrival load distribution $\mu_1 = \mu_2 = 15$, $\sigma_1 = \sigma_2 = 6$. Under the bounded constraint. Observations similar to that for Figure B-6 can be made.

Appendix C

Proofs

C.1. Proof of Proposition 1

The result can be shown by first assuming that all other type 2 agents adopt the conjectured linear strategy, then verifying the first order conditions, and matching terms to obtain the coefficients a^{nc} , b^{nc} , and g^{nc} . There is a unique root that leads to a dynamically stable equilibrium. sequence to converge. expectation method and following the same argument as in

C.2. Proof of Proposition 2

We postulate the value function to be of quadratic form $V^c(x) = A^c x^2 + B^c x$, and plug it in the R.H.S. of the Bellman equation. Solve the minimization problem to get the optimal strategy:

$$u^c(x, d_2) = -\frac{1}{1+A^c}x + \frac{A^c}{1+A^c}d_2 + \frac{A^c}{1+A^c}\mu_1 + \frac{B^c}{2(1+A^c)}$$

Substituting back in the R.H.S., and matching terms on both sides yield the coefficients A^c , B^c , and the optimal per period cost λ^c :

$$\lambda^c = A^c \sigma_1^2 + \frac{A^c}{1 + A^c} q \sigma_2^2 + \mu_1^2 + \frac{1 + A^c - (A^c)^2}{1 + A^c} q \mu_1^2 + 2q \mu_1 \mu_2$$

where

$$A^c = \sqrt{1 - q}, \quad B^c = 2(1 - \sqrt{1 - q})(\mu_2 + \mu_1).$$

Therefore, $(\lambda^c, V^c(x) = A^c x^2 + B^c x)$ forms a solution to the Bellman equation, with the linear optimal stationary strategy $u^c(x, d_2)$ in (3.2).

C.3. Proof of Proposition 3

The stationary distribution of $U(t)$ is of mixed type due to the discrete Poisson arrival and continuous distribution of load realizations. Since the arrival process $\{h_2(t) : t \in \mathbb{Z}\}$ of type 2 agents is exogenous, we first focus on the distribution of the aggregate backlog process $\{x(t) : t \in \mathbb{Z}\}$. When $|a| < 1$, a stationary distribution \mathcal{X} exists and is characterized as follows:

$$\begin{aligned} \mathcal{X} &= \mathcal{X}_k \text{ with probability } q^k(1 - q), \quad (k = 0, 1, \dots) \\ \mathcal{X}_k &= \sum_{i=1}^k a^{i-1} (D_{1,i} + (1 - b)D_{2,i}) + a^k D_{1,k} - \frac{1 - a^k}{1 - a} g \end{aligned}$$

where $\{D_{1,i} : i \in \mathbb{Z}^+\}$ and $\{D_{2,i} : i \in \mathbb{Z}^+\}$ are i.i.d. random sequences respectively.

For every k , the mean and variance of the random variable \mathcal{X}_k are given by:

$$\mathbb{E}[\mathcal{X}_k] = \frac{(1 - a^{k+1})\mu_1 + (1 - a^k)((1 - b)\mu_2 - g)}{1 - a}, \quad \text{Var}[\mathcal{X}_k] = \frac{(1 - a^{2(k+1)})\sigma_1^2 + (1 - a^{2k})(1 - b)^2 \sigma_2^2}{1 - a^2}$$

Under the assumption that $D_{1,i}, D_{2,i} \sim \mathcal{N}(\mu_i, \sigma_i^2)$, $i \in \{1, 2\}$ the load distributions are normal, $\{\mathcal{X}_k : k \in \mathbb{Z}^+\}$ are correlated normal random variables. Note that the mean and variance of \mathcal{X}_k are both increasing in k , we can upper bound the tail probability of \mathcal{X} by the limiting distribution $\lim_{k \rightarrow \infty} \mathcal{X}_k$ as follows:

$$\Pr(\mathcal{X} \geq M) \leq \Pr(\lim_{k \rightarrow \infty} \mathcal{X}_k \geq M)$$

Since $\mathbb{E}[\mathbb{E} \lim_{k \rightarrow \infty} \mathcal{X}_k] = \lim_{k \rightarrow \infty} \mathbb{E}[\mathcal{X}_k]$ and $\lim_{k \rightarrow \infty} \text{Var}[\mathcal{X}_k]$, and it has normal distribution,

$$\Pr(\mathcal{X} \geq M) = 1 - \Phi \left(\frac{M - \frac{\mu_1 + (1-b)\mu_2 - e}{1-a}}{\frac{\sigma_1^2 + (1-b)^2\sigma_2^2}{1-a^2}} \right)$$

C.4. Proof of Proposition 4

The plant G is given by

$$G(s) = \left[\begin{array}{c|cc} \mathbf{A} & \mathbf{B}_1 & \mathbf{B}_2 \\ \hline \mathbf{C}_1 & \mathbf{0} & \mathbf{D}_{12} \\ \mathbf{I} & \mathbf{0} & \mathbf{0} \end{array} \right]$$

where

$$\mathbf{A} = \mathbf{R}_1, \mathbf{B}_1 = \mathbf{R}_2, \mathbf{B}_2 = -\mathbf{R}_1,$$

$$\mathbf{C}_1 = [\mathbf{0} \quad \alpha_2 \mathbf{e} \quad \alpha_3 \mathbf{e}_L]', \mathbf{D}_{12} = [\alpha_1 \mathbf{e} \quad \mathbf{0} \quad -\alpha_3 \mathbf{e}_L]'$$

Consider the feedback gain $\mathbf{F}(s) = \mathbf{D}_K$ that stabilizes the system, the closed loop system is given by

$$\tilde{G}(s) = \left[\begin{array}{c|c} \mathbf{A} + \mathbf{B}_2\mathbf{D}_K & \mathbf{B}_1 \\ \hline \mathbf{C}_1 + \mathbf{D}_{12}\mathbf{D}_K & \mathbf{0} \end{array} \right]$$

$(\mathbf{A} + \mathbf{B}_2\mathbf{D}_K)$ is Hurwitz and $\|\tilde{G}(s)\| < \rho$ if and only iff there exists a symmetric matrix \mathbf{Q} such that:

$$(\mathbf{A} + \mathbf{B}_2\mathbf{D}_K)\mathbf{Q}(\mathbf{A} + \mathbf{B}_2\mathbf{D}_K)' - \mathbf{Q} + \mathbf{B}_1\mathbf{B}_1^* < 0 \quad (\text{C.1})$$

$$\text{Trace}(\mathbf{C}_1 + \mathbf{D}_{12}\mathbf{D}_K)\mathbf{Q}(\mathbf{C}_1 + \mathbf{D}_{12}\mathbf{D}_K)' < \rho \quad (\text{C.2})$$

Denote $\mathbf{P} = \mathbf{D}_K\mathbf{Q}$, note that (C.1), (C.2) are equivalent to:

$$(\mathbf{A}\mathbf{Q} + \mathbf{B}_2\mathbf{P})\mathbf{Q}^{-1}(\mathbf{A}\mathbf{Q} + \mathbf{B}_2\mathbf{P})' - \mathbf{Q} + \mathbf{B}_1\mathbf{B}_1^* < 0$$

$$\text{Trace}(\mathbf{C}_1\mathbf{Q} + \mathbf{D}_{12}\mathbf{P})\mathbf{Q}^{-1}(\mathbf{C}_1\mathbf{Q} + \mathbf{D}_{12}\mathbf{P})' < \rho$$

Also, since trace is monotonic under matrix inequalities, we can find a matrix \mathbf{M} such that $\mathbf{M} < \rho$ and

$$(\mathbf{C}_1\mathbf{Q} + \mathbf{D}_{12}\mathbf{P})\mathbf{Q}^{-1}(\mathbf{C}_1\mathbf{Q} + \mathbf{D}_{12}\mathbf{P})' < \mathbf{M}$$

Apply Schur's complement operation, we have that (C.1), (C.2) are equivalent to the LMIs:

$$\left[\begin{array}{cc} \mathbf{Q} & (\mathbf{A}\mathbf{Q} + \mathbf{B}_2\mathbf{P})' \\ \mathbf{A}\mathbf{Q} + \mathbf{B}_2\mathbf{P} & \mathbf{Q} - \mathbf{B}_1\mathbf{B}_1^* \end{array} \right] > 0, \quad \left[\begin{array}{cc} \mathbf{Q} & (\mathbf{C}_1\mathbf{Q} + \mathbf{D}_{12}\mathbf{P})' \\ \mathbf{C}_1\mathbf{Q} + \mathbf{D}_{12}\mathbf{P} & \mathbf{M} \end{array} \right] > 0.$$

The Pareto optimal strategies can therefore be characterized by the convex optimization problem to minimize ρ with feedback gain $\mathbf{F} = \mathbf{D}_k = \mathbf{Q}\mathbf{P}^{-1}$.

C.5. Proof of Proposition 5

In the non-cooperative setup, the system operator's optimization variables are the pricing parameters \mathbf{q}_1 and \mathbf{q}_2 . We have shown that for given $(\mathbf{q}_1, \mathbf{q}_2)$ pair, at equilibrium agents' load scheduling strategy is the fixed point solution to (4.8). Under the assumption that load arrival process is a i.i.d. sequence, maximizing the system operator's utility is equivalent to minimizing the \mathcal{H}_2 norm of the closed loop system, which is given by the objective in (4.6), where \mathbf{Q} is the controllability Gramian specified by the Lyapunov equation in (4.7).

Appendix D

Supplementary Materials

D.1. Market Architecture Variations for $L = 2$

The tradeoffs we observed between cooperative and non-cooperative schemes also exist in a variety of oligopolistic market architectures. As an example, in this section, we provide two parameterized variations of the market architectures, where the parameter K allows us to tune agents' market power; and parameter θ captures the risk sensitivity of the agents. In these two variations, strategies derived are still of linear forms, with the coefficients as functions of K , and θ , respectively. In the following study of the case with $L = 2$, our focus is the two period dynamics of the representative type 2 agent. For notational convenience, we use m and m^+ to denote $m(t)$ and $m(t + 1)$ for variables $m = x, u, d_1, d_2, p$.

D.1.1 Number of Agents

In the first variation, we adjust agents' market power by scaling the number of type 2 agents in the market. We assume that when $h_2(t) = 1$, K homogeneous type

2 agents, all denoted by $(2, 2)_t$, simultaneously arrive at the market, each of them activates a job with load requirement $d_2(t)/K$ and schedules his consumption over the two periods: $(\nu^K d_2(t)/K, (1 - \nu^K)d_2(t)/K)$. Note that when $K = 1$, it coincides with the case of non-cooperative market architecture. At equilibrium, each type 2 agent solves the problem:

$$\nu^{K,*} = \arg \min_{\nu^K} \left\{ p \frac{d_2}{K} \nu^K + \mathbb{E}_{\{h_2^+, d_2^+, d_1^+\}} \left[p^+ \frac{d_2}{K} (1 - \nu^K) \right] \right\} \quad (\text{D.1})$$

where x is the aggregate backlog state, and price is given by

$$p = x + \frac{d_2}{K} ((K - 1)\nu^{K,*} + \nu^K),$$

$$p^+ = x^+ + d_2^+ \nu^{K,*}.$$

Restricting to linear symmetric equilibria, we obtain an equilibrium strategy as follows:

$$u^K(x, d_2) = \nu^{K,*} d_2 = - \underbrace{\frac{K}{K+1} \frac{1}{(1 + \sqrt{1 - \frac{K}{K+1} q_2})}}_{a^K} x + \underbrace{\frac{1}{1 + \frac{1}{\sqrt{1 - \frac{K}{K+1} q_2}}}}_{b^K} d_2$$

$$+ \underbrace{\frac{\frac{K}{K+1}}{1 + \sqrt{1 - \frac{K}{K+1} q_2}} \left(q_1 \mu_1 + q_2 \mu_2 \frac{1}{1 + \sqrt{1 - \frac{K}{K+1} q_2}} \right)}_{g^K} \quad (\text{D.2})$$

Remark 4 (Limit when $K \rightarrow \infty$) *Even though the agents with flexible loads are price anticipating and behave strategically, as the number of coexisting agents K increases, their market power becomes diluted. When K increases to infinity, the*

equilibrium strategy converges to $u^c(x, d_2)$, the aggregate demand process converges to that of the cooperative scheme. The aggregate cost of all the type 2 agents is minimized, as well as the overall efficiency is maximized in the limit when $K \rightarrow \infty$. At a first glance, this convergence result contradicts to the Cournot limit theorem, which states that in a static partial equilibrium setting of quantity competition, profit maximizing firms become price-takers and the total profits decrease to zero when the number of firms increases to infinity [12]. However, our setup of the dynamic game is different from the Cournot competition in critical ways. Under the marginal cost pricing and deadline constraints, the decisions $u(t)$ from groups of type 2 agents at consecutive periods are strategic complements, while within each group of K identical type 2 agents, their decisions on first period consumption are strategic substitutes. Increasing K leads to higher degree of within group competition which can potentially increase the group's cost in the sense of the Cournot limit theorem; however increasing K also decreases each individual's market power and mitigates the cross group competition, which effect is dominant and overall results in a higher efficiency.

In Figure B-10a we observe that as the market power decreases, market efficiency increases while robustness decreases. In particular, when the agents become price taking as $K \rightarrow \infty$, the first welfare theorem holds and market efficiency is maximized, however the market is at the same time the least robust in terms of demand spikes.

D.1.2 Risk Sensitivity

In the second variation, we consider the case where the agents are risk sensitive, and examine the risk sensitive optimal load scheduling in a cooperative setup. In general, risk averse agents tend to reduce the aggregate demand spikes, at the cost of a larger variance of aggregate demand process.

We follow the Linear-Exponential-Quadratic-Gaussian (LEQG) framework in [26, 14] to study the risk sensitive optimal control. Without loss of generality we assume $q_1 = 1$ and denote $q = q_2$. Under the assumption that the price is proportional to the instantaneous aggregate demand, the risk sensitive objective function is defined recursively as follows:

$$c_t(x, d_2) = q \mathbb{E}_{d_2} \left[(x + u)^2 - \frac{2\beta}{\theta} \log \mathbb{E}_{d_1^+} [e^{-\frac{\theta}{2} c_{t+1}(d_2 - u + d_1^+, d_2^+)}] \right] + (1 - q) \left[x^2 - \frac{2\beta}{\theta} \log \mathbb{E}_{d_1^+} [e^{-\frac{\theta}{2} c_{t+1}(d_1^+, d_2^+)}] \right] \quad (\text{D.3})$$

We also assume the workload distributions Gaussian, namely $D_i \sim \mathcal{N}(\mu_i, \sigma_i^2)$ for $i = 1, 2$. The risk sensitivity is captured by the parameter θ . When $\theta < 0$, the agents are risk averse, and when $\theta > 0$, the agents are risk loving. Note that when $\theta < 0$, the risk averse objective function in (D.3) imposes a larger disutility to large deviations from the mean of $c_{t+1}(x^+, d_2^+)$, leading to higher penalties on the spikes than in the risk neutral formulation. β is the discount factor. As shown in [14], for $\theta < 0$, there is a $\bar{\beta}(\theta)$ ($0 < \bar{\beta} < 1$), such that for $\beta \leq \bar{\beta}(\theta)$, a linear time invariant optimal control policy exists. In our formulation, β is chosen to be a small enough constant to ensure the existence of a solution for the range of θ we consider. Also note that when $\theta \rightarrow 0$, $\bar{\beta}(\theta) \rightarrow 1$, the problem converges to the risk neutral case, and the risk sensitive optimal cooperative strategy converges to that in (3.2). The risk sensitive optimal cooperative strategy minimizes the risk sensitive objective function as follows:

$$u^{c,\theta}(x(t), d_2(t)) = \arg \min_u c_t(x(t), d_2(t))$$

Proposition 6 *For risk sensitivity $\theta \in \mathbb{R}$, there exists a lower bound $\underline{\beta}(\theta)$ and an*

upper bound $\bar{\beta}(\theta)$, such that for $\underline{\beta}(\theta) \leq \beta \leq \bar{\beta}(\theta)$, there exists a risk sensitive optimal cooperative load scheduling strategy of linear form as follows:

$$u^{c,\theta}(x, d_2) = - \underbrace{\frac{1}{1+r_3}}_{a^{c,\theta}} x + \underbrace{\frac{r_3}{1+r_3}}_{b^{c,\theta}} d_2 + \underbrace{\frac{r_3(\mu_1 + \frac{r_1}{2r_2})}{1+r_3}}_{g^{c,\theta}} \quad (\text{D.4})$$

where the coefficients r_i for $i = 1, 2, 3$, are given by:

$$\begin{aligned} r_3 &= \frac{\beta r_2}{1 + \theta \sigma_1^2 r_2} \\ r_2 &= \frac{(1 - \beta - (1 - q)\theta \sigma_1^2) \left(\sqrt{1 + \frac{4(1-q)(\beta + \theta \sigma_1^2)}{(1-\beta - (1-q)\theta \sigma_1^2)^2}} - 1 \right)}{2(\beta + \theta \sigma_1^2)} \\ r_1 &= \frac{2\beta r_2(1 - r_2)(\mu_1 + \mu_2)}{1 + \theta \sigma_1^2 r_2 - \beta(1 - r_2)} \end{aligned}$$

Note that under the cooperative market architecture, when the agents have a risk sensitive objective function as above, the load scheduling strategy derived in (D.4) for $\theta \neq 0$ is different from the risk neutral optimal strategy in (3.2). Nevertheless, system performance measures of efficiency and robustness remain unchanged. In Figure B-10b, we observe that when $\theta \leq 0$ and as the magnitude of θ increases, the agents become more risk averse, and the market efficiency decreases while the robustness increases, and market efficiency achieves the maximum at $\theta = 0$. Moreover, we notice that as the agents become risk loving for $\theta > 0$, their objective deviates from the market efficiency. Load scheduling produces more spikes at the aggregate level, which have large negative impacts that bring down the overall efficiency as well as increase endogenous risks.

D.2. Numerical Study of Classes of Linear Load Scheduling Strategies

Through out this section, we restrict ourselves to linear load scheduling strategies:

$$\mathbf{u}(\mathbf{x}(t)) = \mathbf{F}\mathbf{x}(t),$$

where \mathbf{F} is a $D_c \times D_c$ dimensional matrix.

For general L , the Pareto front cannot be neatly characterized when there are constraints on the feedback controller specified by $\mathbf{u}(t) = \mathbf{F}\mathbf{x}(t)$. Next, we shall numerically examine how the market architectural properties, as reflected by different constraints on \mathbf{F} , affect the location of the corresponding Pareto front.

Intuitively, load scheduling should be operated according to the following principles: firstly, with all other things being equal, an individual demands more resource when his backlog is higher; secondly, when other agents' backlog states are high, he forms the rational expectation that the instantaneous cost will be driven up, thus he consumes less to avoid the high instantaneous price. These are consistent with all the linear strategies we have examined for the case $L = 2$, which are of the form $u(x, d_2) = -ax + bd_2 + g$ where $a > 0, b > 0$. Based on the above intuition, we consider the following constraint sets:

- $\mathcal{F}_{DL} \triangleq \{\mathbf{F} \in \mathbb{R}^{D_c \times D_c} : \mathbf{F}_{(l,1)} = \mathbf{e}_{(l,1)}, \forall l \in \mathcal{L}\}$, where $\mathbf{F}_{(l,1)}$ is the row vector corresponding to the strategy of agent $(l, 1) \in \mathcal{C}$, who meets his deadline, and $\mathbf{e}_{(l,1)}$ is a D_c dimensional row vector with the $(l, 1)$ -th element being one and all others being zero. This is the constraint set in which deadline constraints are enforced.

•

$$\mathcal{F}_\alpha \triangleq \left\{ \mathbf{F} \in \mathbb{R}^{D_c \times D_c} : \begin{array}{l} \mathbf{F}_{(l,\tau),(l,\tau)} = 1, \quad \forall (l,\tau) \in \mathcal{C}, \\ \mathbf{F}_{(l,\tau),(l',\tau')} < 0, \quad \forall (l',\tau') \neq (l,\tau) \in \mathcal{C}, \\ \sum_{(l',\tau') \neq (l,\tau)} F_{(l,\tau),(l',\tau')} = \alpha. \end{array} \right\}$$

for some $\alpha \leq 1$. In this constraint set, an agent's instantaneous demand is negatively proportional to other agent's backlog state, with the sum being α , and his demand is positively proportional to his own backlog with weight 1. When α is small, the agent responds less aggressively to other agents, similar to the non-cooperative load scheduling that we observed in the case with $L = 2$; when α is high, the strategy is similar to the cooperative scheme.

•

$$\mathcal{F}_{BR,\delta} = \left\{ \mathbf{F} \in \mathbb{R}^{D_c \times D_c} : \begin{array}{l} \mathbf{F}_{(l,1)} = \mathbf{e}_{(l,1)}, \quad \forall l \in \mathcal{L} \\ \mathbf{F}_{(l,\tau),(l',\tau')} = \begin{cases} 1 - \delta, & \text{if } (l',\tau') = (l,\tau) \quad \forall 1 < \tau \leq L, l \in \mathcal{L} \\ -\frac{\delta}{D_c - 1}, & \text{if } (l',\tau') \neq (l,\tau) \end{cases} \end{array} \right\}$$

for some $\delta \in [0, 0.5]^1$. This is a parameterized class of *boundedly rational load scheduling strategies*. When the parameter δ is large, individual's load scheduling decision is more sensitive to the other agents' backlog states and less sensitive to his own backlog state. This approximates the scenario when the market architecture facilitates cooperation among agents.

The following corollary shows the impact of δ on aggregate demand volatility and aggregate backlog volatility:

¹ The upperbound on δ is to ensure system stability for each $L \in \mathcal{L}$.

Proposition 7 (Tradeoff of boundedly rational strategy) *Assume that all agents adopt a boundedly rational load scheduling strategy $\mathbf{u}(t) = \mathbf{F}\mathbf{x}(t)$, where $\mathbf{F} \in \mathcal{F}_{BR,\delta}$. The aggregate demand volatility, measured by $\|z_1(t)\|_2^2$ is decreasing in δ , and the backlog volatility, measured by $\|z_2(t)\|_2^2$ is increasing in δ .*

Figure B-9 shows how the total weight that an agent’s linear strategy puts on all other agents’ backlog, i.e. α , affects the Pareto front. We observe that as we decrease α , the Pareto front shifts from the top left corner to the bottom right corner, namely from high efficiency - high risk region to low efficiency - low risk region. This can be viewed as a generalization of our observation in the $L = 2$ case.

D.3. Congestion Fee and Degree of Cooperation

In this example, the system operator can differentiate agents in the market. By imposing a individual specific “congestion fee”, the system operator is able to indirectly adjust the level of cooperation of the market by changing agents’ utility functions.

Recognizing that a key difference between the non-cooperative and the cooperative market architecture is the payoff externality in the dynamic oligopolistic game, we introduce a parameterized payoff function to attenuate the externality. More specifically, for instantaneous price $p(t) = U(t)$, an agent pays for his own demand at the price $p(t)$, and pays for a portion $\gamma(0 \leq \gamma \leq 1)$ of the instantaneous demand from all other agents at the same price $p(t)$. For example, consider a type 2 agent with controllable load $d(t)$, on top of the total cost $p(t)u(t) + p(t+1)(d(t) - u(t))$ for his consumption schedule, he also needs to pay $\gamma p(t)x(t)$, and $\gamma p(t+1)(d_1(t+1) + h_2(t+1)u(t+1))$, during period t and $(t+1)$ ². Note that when $\gamma = 0$, the induced

²There should be an ex-ante money transfer from type 1 agents to type 2 agents in order to prevent type 2 agents from mimicing type 1 agents. However we do not explicitly calculate the

strategy is the same as that under the original non-cooperative market architecture; and when $\gamma = 1$, the equilibrium strategy is close to, though not equivalent to, the cooperative strategy where there is no payoff externality among the agents.

With the level of payoff externality parameterized by γ , the equilibrium load scheduling strategy is given by solving the following fixed point equation

$$u^\gamma(x, d_2) = \arg \min_u \left\{ p(u + \gamma x) + \mathbb{E}_{\{h_2^+, d_2^+, d_1^+\}} [p^+(d_2 - u + \gamma (d_1^+ + h_2^+ u^\gamma(x^+, d_2^+)))] \right\} \quad (\text{D.5})$$

where $p(t) = U(t)$, and $x^+ = d_2 - u + d_1^+$. The equilibrium strategy is given by:

$$u^\gamma(x, d_2) = -a^\gamma x + b^\gamma d_2 + g^\gamma \quad (\text{D.6})$$

where the coefficients a^γ , b^γ , and g^γ given by the following system of equations:

$$\begin{cases} \gamma q (a^\gamma)^3 - (1 + \gamma) q (a^\gamma)^2 + 2a^\gamma - \frac{1+\gamma}{2} = 0 \\ b^\gamma = 1 - \frac{2a^\gamma}{1+\gamma} \\ qg^\gamma = \frac{[(1-q)(1+\gamma) - q(2\gamma a^\gamma - 1 - \gamma)(1 - a^\gamma)]\mu_1 - q(2\gamma a^\gamma - 1 - \gamma)b^\gamma \mu_2}{q(2\gamma a^\gamma - 1 - \gamma) + \frac{1+\gamma}{a^\gamma}} \end{cases}$$

We evaluate the market efficiency and the upper bound of risk for $\gamma \in [0, 1]$. In Figure B-11, we can observe the efficiency-risk tradeoff. As we increase γ from 0 to 1, the level of payoff externality decreases, and market efficiency increases while robustness decreases, both monotonically.

amount of initial transfer for screening purpose, we shall instead focus on the equilibrium strategy of type 2 agents, and examine how the aggregate behavior affects the efficiency-risk tradeoffs at the macro level.

D.4. Example of state space model of LTI system for $L = 3$

As an example, for $L = 3$ and the two outputs that we measure are:

$$z_1(t) = [1 \ 1 \ 1 \ 1 \ 1 \ 1] \mathbf{F} \mathbf{x}(t)$$

$$z_2(t) = [1 \ 1 \ 1 \ 1 \ 1 \ 1] \mathbf{x}(t)$$

The constant matrices \mathbf{R}_1 , \mathbf{R}_2 , and $\mathbf{F} \in \mathcal{F}_{BR,\delta}$ are given by:

$$\mathbf{R}_1 = \begin{bmatrix} 0 & 0 & 0 & 0 & 0 & 0 \\ 0 & 0 & 0 & 1 & 0 & 0 \\ 0 & 0 & 0 & 0 & 1 & 0 \\ 0 & 0 & 0 & 0 & 0 & 0 \\ 0 & 0 & 0 & 0 & 0 & 1 \\ 0 & 0 & 0 & 0 & 0 & 0 \end{bmatrix}, \quad \mathbf{R}_2 = \begin{bmatrix} 1 & 0 & 0 \\ 0 & 0 & 0 \\ 0 & 0 & 0 \\ 0 & 1 & 0 \\ 0 & 0 & 0 \\ 0 & 0 & 1 \end{bmatrix},$$

$$\mathbf{F} = \begin{bmatrix} 1 & 0 & 0 & 0 & 0 & 0 \\ 0 & 1 & 0 & 0 & 0 & 0 \\ 0 & 0 & 1 & 0 & 0 & 0 \\ -\frac{\delta}{5} & -\frac{\delta}{5} & -\frac{\delta}{5} & 1 - \delta & -\frac{\delta}{5} & -\frac{\delta}{5} \\ -\frac{\delta}{5} & -\frac{\delta}{5} & -\frac{\delta}{5} & -\frac{\delta}{5} & 1 - \delta & -\frac{\delta}{5} \\ -\frac{\delta}{5} & -\frac{\delta}{5} & -\frac{\delta}{5} & -\frac{\delta}{5} & -\frac{\delta}{5} & 1 - \delta \end{bmatrix},$$

Bibliography

- [1] R. Belhomme, R.C.R. De Asua, G. Valtorta, A. Paice, F. Bouffard, R. Rooth, and A. Losi. Address-active demand for the smart grids of the future. In *SmartGrids for Distribution, 2008. IET-CIRED. CIRED Seminar*, pages 1–4. IET, 2008.
- [2] D.P. Bertsekas. *Dynamic programming and optimal control 3rd edition, volume ii*. 2011.
- [3] R. Buyya and M. Murshed. A deadline and budget constrained cost-time optimisation algorithm for scheduling task farming applications on global grids. *Arxiv preprint cs/0203020*, 2002.
- [4] R. Buyya, C.S. Yeo, and S. Venugopal. Market-oriented cloud computing: Vision, hype, and reality for delivering it services as computing utilities. In *High Performance Computing and Communications, 2008. HPCC'08. 10th IEEE International Conference on*, pages 5–13. Ieee, 2008.
- [5] J. Chae. Trading volume, information asymmetry, and timing information. *The Journal of Finance*, 60(1):413–442, 2005.

- [6] A.I. Cohen and C.C. Wang. An optimization method for load management scheduling. *Power Systems, IEEE Transactions on*, 3(2):612–618, 1988.
- [7] Romain Couillet, Samir Medina Perlaza, Hamidou Tembine, and M erouane Debbah. A mean field game analysis of electric vehicles in the smart grid. In *Computer Communications Workshops (INFOCOM WKSHPS), 2012 IEEE Conference on*, pages 79–84. IEEE, 2012.
- [8] J. Danielsson and H.S. Shin. Endogenous risk. *Modern risk management: A history*, pages 297–316, 2003.
- [9] J. Danielsson, H.S. Shin, and J.P. Zigrand. Endogenous and systemic risk, 2011.
- [10] J.M. Foster and M.C. Caramanis. Energy reserves and clearing in stochastic power markets: The case of plug-in-hybrid electric vehicle battery charging. In *Decision and Control (CDC), 2010 49th IEEE Conference on*, pages 1037–1044. IEEE, 2010.
- [11] J. Geanakoplos. *The leverage cycle*. Yale University, Cowles Foundation for Research in Economics, 2009.
- [12] E.J. Green. *Non-cooperative price taking in large dynamic markets*. Econometric Research Program, Princeton University, 1978.
- [13] S.J. Grossman and J.E. Stiglitz. On the impossibility of informationally efficient markets. *The American Economic Review*, 70(3):393–408, 1980.
- [14] L.P. Hansen and T.J. Sargent. Discounted linear exponential quadratic gaussian control. *Automatic Control, IEEE Transactions on*, 40(5):968–971, 1995.

- [15] T.T. Kim and H.V. Poor. Scheduling power consumption with price uncertainty. *Smart Grid, IEEE Transactions on*, 2(3):519–527, 2011.
- [16] W. Leontief. Stackelberg on monopolistic competition. *The Journal of Political Economy*, 44(4):554–559, 1936.
- [17] C. Li and L. Li. Utility-based scheduling for grid computing under constraints of energy budget and deadline. *Computer Standards & Interfaces*, 31(6):1131–1142, 2009.
- [18] E. Maskin and J. Tirole. A theory of dynamic oligopoly, iii: Cournot competition. *European Economic Review*, 31(4):947–968, 1987.
- [19] E. Maskin and J. Tirole. A theory of dynamic oligopoly, i and ii. *Econometrica: Journal of the Econometric Society*, pages 549–569, 1988.
- [20] A.H. Mohsenian-Rad and A. Leon-Garcia. Optimal residential load control with price prediction in real-time electricity pricing environments. *Smart Grid, IEEE Transactions on*, 1(2):120–133, 2010.
- [21] C. Nottola, F. Leroy, and F. Davalo. Dynamics of artificial markets. In *Toward a practice of autonomous systems: proceedings of the First European Conference on Artificial Life*, page 185. MIT Press, 1994.
- [22] M. Roozbehani, M.I. Ohannessian, M. Donatello, and M.A. Dahleh. Load-shifting under perfect and partial information: Models, robust policies, and economic value. *Submitted to Operations Research*.
- [23] F.C. Schweppe. *Spot pricing of electricity*. Springer, 1988.

- [24] L.S. Shapley. Stochastic games. *Proceedings of the National Academy of Sciences of the United States of America*, 39(10):1095, 1953.
- [25] R.A. Stubbs and D. Vandebussche. Multi-portfolio optimization and fairness in allocation of trades. 2009.
- [26] P. Whittle and P.R. Whittle. *Risk-sensitive optimal control*. Wiley Chichester, 1990.